Giant dipole resonance in ^{17}O observed with the (γ,p) reaction

D. Zubanov and M. N. Thompson

School of Physics, University of Melbourne, Parkville, Victoria 3052, Australia

B. L. Berman

Center for Nuclear Studies, Department of Physics, The George Washington University,
Washington, D.C. 20052

J. W. Jury

Department of Physics, Trent University, Peterborough, Ontario, Canada K9J 7B8

R. E. Pywell

Accelerator Laboratory, University of Saskatchewan, Saskatoon, Saskatchewan, Canada S7N 0W0

K. G. McNeill

Department of Physics, University of Toronto, Toronto, Ontario, Canada M5S 1A7

The giant dipole resonance (GDR) in ^{17}O has been studied with the reaction $^{17}O(\gamma,p)^{16}N$ from $E_\gamma = 13.50$ to 43.15 MeV using quasimonoenergetic photons. The measured cross section shows major peaks at 15.1, 18.1, 19.3, 20.3, 22.2, 23.1, 24.4, and ~ 26.5 MeV. The intermediate structure in the main GDR region is remarkably similar to that observed in ^{16}O, indicating that the valence neutron outside the doubly magic ^{16}O core perturbs the core-excited states minimally, in support of the weak-coupling hypothesis. We correlate the trends in GDR structure of $^{16,17,18}O$ with changes in ground-state properties related to static deformation. The (γ,p) reaction selects strength predominantly from two-particle–one-hole configurations formed via $E1$ transitions from the $1p_{1/2}$ subshell; comparison with other reactions (photoneutron and radiative capture) provides information on the microscopic structure of $E1$ states. The peak observed near threshold at 15.1 MeV is remarkably strong; we infer that it originates from photoexcitation of a few narrow $T=\frac{3}{2}$ states and that $M1$ transitions contribute to the measured strength. The total absorption cross section is approximated by summing the (γ,p) cross section and the previously published photoneutron cross section; comparison with particle-hole shell-model calculations shows that the main cross-section features, including isospin distribution, are well predicted. Evidence is found for isospin splitting in ^{17}O. Systematics of the integrated cross sections for the carbon, nitrogen, and oxygen isotopes are delineated.

PACS number(s): 24.30.Cz, 25.20.Lj, 27.20.+n

I. INTRODUCTION

The very loose binding (4.14 MeV) of the $1d_{5/2}$ valence neutron to the doubly magic ^{16}O core makes the ^{17}O nucleus perhaps the ideal case to observe the influence of a weak perturbation on the $E1$ core-excited states forming the giant dipole resonance (GDR). The photoneutron cross section for ^{17}O has been measured [1] and shows evidence of some intermediate structure in the GDR region, the details of which are not sufficiently clear to establish their relationship with the sharp intermediate structures clearly visible in the photonuclear cross sections of ^{16}O [2]. The photoproton reaction on ^{17}O is a particularly suitable means of probing the effects of the valence neutron on the core-excited GDR states since it involves transitions only from the core and excludes strength from the valence neutron. In addition, the structure in this reaction should be more pronounced than that in the photoneutron cross section since far fewer reaction channels are represented. This paper reports the first measurement of the $^{17}O(\gamma,p)^{16}N$ cross section.

This reaction probes the simple particle-hole structure of the core-excited states. The final states of ^{16}N populated via the photoproton reaction are known [3] to have a very pure one-particle–one-hole (1p-1h) nature with strong $(1p_{1/2})^{-1}$ components. The photoproton reaction mechanism in light nuclei is dominated by the semidirect process [4] (i.e., direct decay of the intermediate GDR state), which has been recently confirmed for ^{17}O [5]. This reaction then selects the 2p-1h configurations with $(1p_{1/2})^{-1}$ components in the wave function of the intermediate states, whereas the photoneutron cross section contains strength from 2p-1h and more complex configurations dominated by $(1p_{3/2})^{-1}$ components. Comparison of the cross sections should allow identification of strong 2p-1h features and indicate the relative importance of $(1p_{1/2})^{-1}$ and $(1p_{3/2})^{-1}$ components.

Reactions involving radiative capture of composite particles, $^{14}C(^3He,\gamma)^{17}O$ and $^{14}N(^3H,\gamma)^{17}O$, have been reported [6,7] and show resonances in the region of the GDR. These reactions probe the 3p-2h components of the continuum wave function [8]. Hence it would be use-

ful to compare these results with those of the present measurement in order to see the relative importance of 2p-1h and 3p-2h configurations in the GDR region of ^{17}O. This is interesting particularly since multiparticle-multihole (2p-2h, 3p-3h, etc.) components are thought to play an important role in the formation of intermediate structure observed in ^{16}O [8,9].

In the weak-coupling model [10], the photoabsorption cross section for ^{17}O consists of a component corresponding to the excitations of the valence neutron, with the core remaining inert, plus strength from excitations of the ^{16}O core, with the valence neutron acting as a spectator. The strength from valence neutron excitations can be identified with the classic pygmy resonance observed in the photoneutron cross section of ^{17}O at ~ 13.5 MeV, below the main GDR strength (~ 23 MeV) [1]. Its absence in ^{16}O suggests that this strength may be associated with the valence neutron. Its formation via single-particle excitation of the valence neutron leaving the residual core in its ground state is supported by the measurements [11,12] of the (γ,n_0) cross section, which accounts for most of the photoneutron strength in the region of the pygmy resonance. This illustrates the minor role of the core in valence neutron excitations. One then has good reason to expect that the valence neutron plays a minor role in core excitations, particularly since these are at a higher energy. Some support for this comes about from the observation that the gross features of the main GDR strength in ^{17}O, i.e., its location, shape, and width, are similar to those in ^{16}O, indicating that the coupling of the valence neutron to the core is too weak to disrupt the GDR in a major way. The present measurement provides a more stringent test of the validity of the weak-coupling picture for the ^{17}O nucleus in the GDR region since it provides a clearer view of the intermediate structure.

The particle-hole shell model should provide a good framework for the description of $E1$ states in ^{17}O especially since the gross features of the ^{16}O photoabsorption cross section are well predicted in the 1p-1h model [13] and the weak-coupling picture seems to hold. Several particle-hole model calculations [14–17] of the photoabsorption cross section for mass-17 nuclei have been carried out in the 2p-1h and 1p basis differing mainly in the form of the residual two-body nucleon-nucleon interaction that was used. It is of interest to see how well these calculations perform in a truncated shell-model basis and, within this truncation, to note which form of the residual interaction gives best agreement with experiment.

The first such calculation of the $E1$ strength distribution was performed for the mirror ^{17}F nucleus by Harakeh, Paul, and Gorodetzky [14] using the realistic Kuo-Brown interaction. The only photonuclear data for mass-17 nuclei available at that time for comparison with the model predictions was their ^{17}F$(\gamma,p_0)^{16}$O cross section [14] (15.4–30.4 MeV) obtained using the principle of detailed balance from the ^{16}O$(p,\gamma_0+\gamma_1)^{17}$F 90° excitation function. This reaction is $T=\frac{1}{2}$ selective (assuming isospin is a good quantum number) and reflects only part of the total $T=\frac{1}{2}$ distribution in the GDR and so was useful for assessing the predictions of the $T=\frac{1}{2}$ strength only.

Two additional calculations were reported by Albert et al. [16], one using the Soper interaction and another using the Tabakin interaction. Again, only the ^{17}F$(\gamma,p_0)^{16}$O reaction data were available for comparison with the calculated $T=\frac{1}{2}$ distribution.

More data for the $T=\frac{1}{2}$ states became available later with the measurement of the differential cross section at 98° for the ^{17}O$(\gamma,n_0)^{16}$O reaction (5.0–30.4 MeV) by Johnson et al. [11] and the integrated-over-angles cross section and angular distributions for the same reaction (10.1–24.0 MeV) by Jury et al. [12].

The first investigation of the main GDR strength in ^{17}O was carried out by Norum, Bergstrom, and Caplan [15] via inelastic electron scattering (at 75°). Their results defined the broad features of the GDR, but are limited for comparison with the above predictions because of the presence of multipolarities other than $E1$ and of isoscalar strength. They also performed a particle-hole calculation of the differential $C1$ form factors using both the Boeker-Brink and Kuo-Brown interaction and find that the latter provides a far better description of the strength distribution observed in their spectra and the q dependence of the GDR.

The measurement of the photoneutron cross section for ^{17}O by Jury et al. [1] provided the first photonuclear data for the core-excited states. Comparison was made with results of Albert et al. [16] only. More recently, another calculation, by Eden and Assafiri [17], using the Cooper-Eisenberg interaction has been carried out expressly to calculate core-excited states in the 2p-1h framework, excluding 1p-0h excitations.

The present data permit a more complete evaluation of these calculations than was possible with previous data, particularly since it can be summed with the photoneutron cross section to obtain a good approximation of the photoabsorption cross section for ^{17}O.

The photoabsorption cross section for ^{17}O consists of two isospin components $T_< = \frac{1}{2}$ and $T_> = \frac{3}{2}$, formed via isovector transitions from the $T=\frac{1}{2}$ ground state of ^{17}O. The energy distribution of these two components and their properties—such as the relative intensity and displacement energy between the centers of strength of the two components (isospin splitting magnitude)—provides further tests of the shell-model predictions and various other estimates of the properties of these distributions. Of particular interest is the phenomenon of isospin splitting, which has been established in heavy nuclei [18]. In light nuclei the situation is more complex since the two distributions generally overlap. A special case is the ^{13}C nucleus which provides a good example of isospin splitting [19]: A strong 2p-1h $T_<$ fragment is observed at 21 MeV below the main $T_>$ GDR at ~ 24.5 MeV. Such clear separation has not been reported in ^{17}O. Experimental evidence for this phenomenon in ^{17}O is still lacking. Estimates of its magnitude [14,21,22] are roughly one-half of the GDR width (~ 6 MeV), so that strong overlap of the two groups is expected, thus making it difficult to determine their energy distributions. By identifying the resonances in the GDR and their isospin nature, it might then be possible to distinguish the two

groups.

This measurement is part of a series [23] (*C-N-O* aimed at measuring the (γ, n_0), $(\gamma, 1n)$, $(\gamma, 2n)$, and (γ, p) cross sections for neutron-rich isotopes of carbon (^{13,14}C), nitrogen (^{15}N), and oxygen (^{17,18}O), which may be considered to have one or two particles or holes outside an $A = 4n$ core (^{12}C or ^{16}O). The recent measurement [24] of the ^{14}C(γ, p) cross section, made subsequent to this measurement, completes the carbon series. The present measurement completes the oxygen series and allows us to observe for the first time the effects of progressively adding neutrons to the doubly magic ^{16}O core on the core-excited GDR states. A short summary of the systematic trends observed in the carbon and oxygen isotopes is presented in Ref. [24].

II. EXPERIMENTAL DETAILS

A. Photon source

The experiment was performed at the Lawrence Livermore National Laboratory (LLNL) Electron-Positron Linear Accelerator Facility using a beam of quasi-monoenergetic photons produced from positron annihilation in flight. A brief description of this facility is given below; further details are available elsewhere [25–29].

A 120-MeV electron beam from the linac, pulsed at 720 Hz, was directed onto a tungsten-rhenium converter where fast positrons were created from electron bremsstrahlung by pair production. These positrons were transported through an analyzing slit, set to restrict the momentum spread of the beam to $\pm 1\%$. The analyzed beam, having typical currents of ~ 1 nA (at $E_\gamma = 24$ MeV), was then focused onto a 0.76-mm-thick beryllium disk of diameter 12.7 mm. A small fraction of the positrons in the beam interact in the target to produce a nearly monoenergetic spectrum of photons by annihilation, as well as a continuous spectrum of bremsstrahlung photons. The transmitted positrons were magnetically deflected through 90° into a 5-m-deep beam dump. The forward moving photon beam then passed through a series of circular collimators and a well-shielded photon-flux monitor before striking the ^{17}O sample, which was positioned 3.1 m from the annihilation target and directly in line with the positron beam. The collimation was designed so that the beam diameter was fractionally greater than that for the sample, which is usually fixed at 3.81 cm for experiments at this facility.

Because the photon beam includes both annihilation and bremsstrahlung photons, the measured yield at a given positron energy does not give a direct measure of the cross section: Correction for the bremsstrahlung contribution must be made. This was done by repeating yield measurements with a photon beam derived from electrons instead of positrons and subtracting this contribution, after appropriate normalization, from the yield measured with the positron-generated beam. The energy resolution [full width at half maximum (FWHM)] of the annihilation-photon spectrum, as a result mainly of the positron energy spread and energy loss in the annihilation target, was ~ 320 keV at $E_\gamma = 15$ MeV [30] and increased

in a near-linear way [25,31] to ~ 400 keV at $E_\gamma = 30$ MeV. The energy calibration had been determined to an accuracy of about $\pm 0.25\%$ in previous experiments [26–29,32] by the observation of several $(\gamma, 2n)$ reaction thresholds, resonances in the ^{16}O(γ, n) cross section, and the 15.11-MeV state in the ^{13}C(γ, n) cross section [33].

B. Detection system

The ^{17}O$(\gamma, p)^{16}$N cross section was derived from the yield of ^{16}N activity, measured as a function of positron energy. The residual ^{16}N decays by β^- emission with a half-life of 7.13 s. Transitions to excited states in ^{16}O lead to emission of 6.13- and 7.12-MeV γ rays, which result, respectively, from 67.0% and 4.9% of the β^- decays [34]. The remaining decays are almost entirely to the ground state of ^{16}O, resulting in a spectrum of β^- particles with an end-point energy of 10.42 MeV [34]. This short-lived ^{16}N activity was detected between linac beam bursts in the experimental arrangement described below. The dominant 6.13-MeV γ-ray branch forms the basis of the present measurement.

The 6.13-MeV γ rays were detected efficiently *in situ*, using two large NaI(Tl)-crystal spectrometers, one 27.94 cm diameter $\times$ 13.97 cm and the other 20.32 cm $\times$ 20.32 cm. These spectrometers were positioned close to the sample, in a horizontal plane, with the axis of each crystal at 90° relative to the incident beam direction. With the exception of the front face, each spectrometer was shielded by 10 cm of lead. For the front face, a 17.8-cm-diam collimator hole was cut in the 2.5-cm-thick lead shielding. Further shielding was provided by boric-acid bricks to reduce the activation of NaI crystals by the intense flux of thermal neutrons produced during the 3-μs-long beam burst.

Each NaI crystal was viewed by four photomultiplier tubes (PMT's), the gains of which were carefully matched. The output signals were summed, amplified, and shaped and then fed into a programmable pulse-height analyzer. For data taken below $E_\gamma = 29$ MeV, the analyzer was gated to ensure that pulses produced more than 65 μs after the beam burst were analyzed, thus giving a gating efficiency of 95%. Above $E_\gamma = 29$ MeV the gate delay was increased to 140 μs in order to minimize spectrum-resolution deterioration resulting from short-term PMT gain instabilities which were induced by a significant increase of the background in the detectors during the beam burst.

The efficiency for detection of 6.13-MeV γ rays from the extended ^{17}O sample was determined using spectra collected from a calibrated [35] ^{238}Pu-α-^{13}C source positioned at several locations along the sample axis. The 6.13-MeV γ rays from this source result from the ^{13}C$(\alpha, n)^{16}$O reaction, which populates the same (second) excited state in ^{16}O as that which is populated following β^- decay from the ^{16}N formed by the ^{17}O(γ, p) reaction [34]. In determining the absolute cross-section scale, it is necessary to have at least one detector calibrated absolutely, and we used the 27.94 cm $\times$ 13.97 cm NaI spectrometer for this purpose; its better resolution allowed for a more reliable extraction of the 6.13-MeV γ-ray photo-

peak area. The photopeak efficiency for the extended sample was determined by taking into account (i) the variation of the photopeak efficiency along the sample axis, (ii) the reduction in the ^{16}N activity along the length of the sample as a result of attenuation of the incident beam by the sample, and (iii) a correction of 5% for the self-absorption of γ rays, calculated by a Monte Carlo method [36]. This efficiency was confirmed by another result obtained by multiplying the total efficiency calculated for the present geometry using the Monte Carlo code [36] by the peak-to-total ratio determined from sample spectra measured in this experiment.

C. Sample details

The sample consisted of 52.0 g of ^{17}O in the form of isotopically enriched water, in two parts [H_2^{17}O (I) and (II)], with different isotopic compositions as detailed in Table I. Each part was contained in a separate thin-walled Lucite [$(C_5H_8O_2)_n$] cylinder, 3.81 cm in diameter and of length as indicated in Table I.

The ^{18}O contaminant in this sample, amounting to 31.1 g, contributed to the ^{16}N activity via the ^{18}O(γ,pn) and ^{18}O(γ,d) reactions. This contribution to the ^{17}O(γ,p) reaction yield was measured by irradiating an ^{18}O-enriched water sample containing 83.3 g of ^{18}O, also in two cylinders [H_2^{18}O (I) and (II)] with different isotopic compositions and lengths as detailed in Table I. This necessary background determination provided the only available measurement of the ^{18}O((γ,pn)+(γ,d)) reaction cross section, which is reported elsewhere [20].

The beam-dependent background was measured by irradiating a sample of distilled water also packaged in two separate cylinders [H_2^{nat}O (I) and (II)]. The H_2^{nat}O, H_2^{17}O, and H_2^{18}O samples were each held in identical styrofoam containers to facilitate pneumatic transfer into and out of the beam.

A remotely controlled pneumatic device was used to place the various samples in a reproducible location between the NaI detectors. This device was aligned optically so that the beam line, defined by the centers of the annihilation target and collimators, passed through the center of the sample; we believe that the umbra of the beam covered the entire sample.
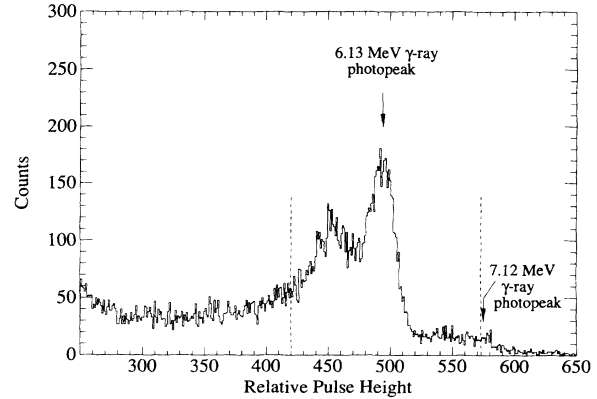

FIG. 1. H_2^{17}O-sample spectrum (27.94 cm $\times$ 13.97 cm NaI) collected for 20 min at E_γ = 35 MeV with the positron beam incident on the annihilation target. The markers indicate the summation region 5.2–7.1 MeV that was used in the analysis. The lower limit was chosen to exclude the long-lived beam-induced background present in the spectra below 5.2 MeV. The upper limit was chosen to minimize the effects of any error in the energy calibration ($\lesssim \pm 0.3\%$) on the sum of events between the markers.

D. Photon-flux monitoring

The photon flux was measured using a calibrated [26] cylindrical transmission ion chamber filled with xenon gas. The stability of this chamber was monitored periodically during the experiment by placing a ^{60}Co γ-ray source in a standard position near the chamber; drifts in the ion-chamber response were negligible ($\lesssim 0.5\%$). The chamber background, resulting from cosmic rays and electronic noise, also was measured periodically. Continuous monitoring of the photon-flux rate during the irradiation period was achieved by recording the digitized flux in 1-s intervals. This time spectrum, representing the photon-flux history, also facilitated a small correction for that part of the ^{16}N activity that remained after the irradiation period and which was not recorded because of a large increase in PMT gain immediately after the beam was switched off.

TABLE I. Characteristics of the samples used in the present measurements.

Sample		Mass (g)	Length (cm)	Isotopic composition (at. %)[a]		
				^{16}O	^{17}O	^{18}O
H_2^{17}O	(I)	79.3	6.6	18.2	45.3	36.5
	(II)	40.8	3.5	34.62	54.75	10.63
H_2^{18}O	(I)	72.7	5.8	2.77	1.86	95.37
	(II)	23.9	1.9	2.5	1.4	96.1
H_2^{nat}O	(I)	74.5	6.6	99.762	0.038	0.200
	(II)	34.1	3.0	99.762	0.038	0.200

[a]The isotopic compositions for the enriched-water samples were provided by Monsanto Research Corporation, Mound Facility, Miamisburg, OH.

E. Data acquisition

The annihilation-photon energy was varied from 13.50 MeV (just below the 13.78-MeV reaction threshold [37]) to 43.15 MeV. For each positron-energy setting, spectra were collected, in turn, from the irradiated composite samples of $H_2^{nat}O$, $H_2^{17}O$, and $H_2^{18}O$. The spacing between successive positron-irradiation energies was varied from 120 keV near threshold to 960 keV at photon energies above $E_\gamma = 29$ MeV. In order to measure the positron bremsstrahlung contribution to the yield, data were collected with the electron beam incident on the annihilation target. These data were taken with coarser energy spacings than those taken using annihilation photons.

With $H_2^{nat}O$, $H_2^{18}O$, and $H_2^{17}O$ samples in position, minimum counting periods for energies above $E_\gamma = 29$ MeV were 10, 20, and 30 min, respectively. These periods were increased up to 60 min for energies below $E_\gamma = 29$ MeV. A pulse-height spectrum from the $H_2^{17}O$ sample is shown in Fig. 1.

III. DATA ANALYSIS AND EXPERIMENTAL UNCERTAINTIES

A. Reduction of data to absolute cross section

At each photon energy, the number of $^{17}O(\gamma,p)$ reaction events was determined from the sum of counts in the $H_2^{17}O$-sample spectrum between 5.2 and 7.1 MeV as indicated in the spectrum shown in Fig. 1. Before summing, each spectrum was energy calibrated to compensate for long-term gain drifts in the PMT which may have occurred during the experiment. This number of events was then corrected for (i) the gating factor (1.05 for $E_\gamma < 29$ MeV and 1.11 for $E_\gamma \geq 29$ MeV); (ii) the dead-time factor, determined by taking the ratio of real to live time ($< 1.5\%$); (iii) the beam-independent background, determined precisely over many hours ($\sim 40\%$ at $E_\gamma \simeq 15$ MeV, $\sim 12\%$ at $E_\gamma \simeq 23$ MeV, and $\lesssim 3.5\%$ for $E_\gamma \gtrsim 30$ MeV); and (iv) the ^{16}N activity remaining after the irradiation period, but which was not counted (accurate corrections, of $< 2\%$, were made on the basis of the recorded photon-flux history). Spectra from the $H_2^{nat}O$ and $H_2^{18}O$ samples were reduced in a similar way.

The relative reaction yield then was determined at each photon energy by dividing the corrected number of events (N) by the photon flux (Q). The flux was corrected for the ion-chamber background, resulting primarily from cosmic rays and from electronic noise in the current-to-frequency converter. The contribution of this background to the total measured flux was $\sim 25\%$ at $E_\gamma \simeq 15$ MeV, $\sim 11\%$ at $E_\gamma \simeq 23$ MeV, and $\lesssim 3\%$ for $E_\gamma \gtrsim 30$ MeV.

This procedure, after having been repeated for every point, reduced the data to six complete yield curves for each detector: one yield curve with positrons incident on the annihilation target and one with electrons incident for each of the three samples. These yield curves for each detector were analyzed independently following the procedure outlined below.

The $H_2^{nat}O$-sample yields represent the total beam-dependent background which originates from reactions induced by the photon beam ($\sim 70\%$) mainly in the collimators and by the $e^\pm$ beam ($\sim 30\%$) mainly in the beam dump; the presence of the $H_2^{nat}O$ sample accounts for $\lesssim 10\%$ of the total measured background. These background yields are nearly constant across the entire energy range spanned in the experiment. A linearly fitted value was therefore subtracted at each energy from the $H_2^{17,18}O$-sample yields to obtain yields representing contributions from $^{17,18}O$ alone. This background accounts for 8%, 6%, and 4% of the $H_2^{17}O$-sample yield measured with positrons incident on the annihilation target at $E_\gamma = 15$, 22, and 40 MeV, respectively.

The $^{17,18}O$-sample yields which result from annihilation photons alone were determined by subtracting the electron-run yields from the positron-run yields:

$$\left[\frac{N}{Q}\right]_n = \left[\frac{N}{Q}\right]_n^{e^+} - k \left[\frac{N}{Q}\right]_n^{e^-} \quad (n = 17, 18) , \qquad (1)$$

where k is the previously measured [26,28] energy-dependent normalization factor which allows for the different photon-flux monitor response for positrons and electrons. Since the electron-run data were taken in larger energy steps than the positron-run data, it was necessary to smooth the electron-run yield curve and interpolate to obtain the yield at appropriate energies. Figure 2 shows a comparison of the positron-run yield from the $H_2^{17}O$ sample with the normalized electron-run yield (and its smooth representation) using the 27.94 cm $\times$ 13.97 cm NaI detector.

The net yield $(N/Q)^{net}$ due to the $^{17}O(\gamma,p)$ reaction alone was obtained by removing the contribution of the ^{18}O contaminant in the $H_2^{17}O$ sample as follows:

$$\left[\frac{N}{Q}\right]^{net} = m_{17}G_{17}\left[\frac{N}{Q}\right]_{17} - r_\varepsilon m_{18}G_{18}\left[\frac{N}{Q}\right]_{18} . \qquad (2)$$

Here $m_{18} = 0.38$ ($m_{17} = 1.01$) is the mass normalization constant which corrects for the presence of ^{18}O (^{17}O) in
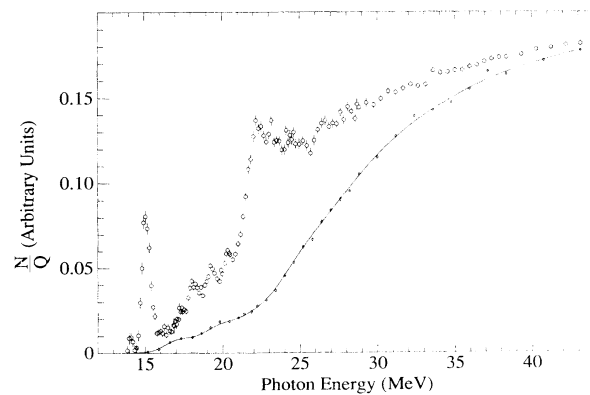

FIG. 2. Yield from the $H_2^{17}O$ sample and the 27.94 cm $\times$ 13.97 cm NaI detector obtained with positrons incident on the annihilation target, compared with the normalized yield (and its smooth representation) obtained when electrons are used.

the $H_2^{17}O$ ($H_2^{18}O$) sample; G_{17} (G_{18}) corrects for the atomic attenuation of photons in passing through the $H_2^{17}O$ ($H_2^{18}O$) sample and varies from 1.11 (1.08) at threshold to 1.09 (1.07) at $E_\gamma = 43$ MeV; $r_\varepsilon = 0.98$ and is the ratio of efficiency for detection of ^{16}N activity from the $H_2^{17}O$ sample to that from the $H_2^{18}O$ sample. The uncertainties in these factors are small and result in a negligible uncertainty in the cross section.

Figure 3 shows for each detector the H_2^{17}O-sample yield at this stage of the analysis compared with the H_2^{18}O-sample yield, where the yields have been scaled by the factors given in Eq. (2). The observed structure in these yields reflects directly the structure in the cross sections. The yield from the H_2^{18}O sample is due to both the $^{18}O(\gamma,pn)$ reaction (above 21.82 MeV) and the $^{18}O(\gamma,d)$ reaction (above 19.60 MeV). Below these thresholds the nonzero yield has been identified as being due to capture of fast neutrons by the NaI crystals. These neutrons result from delayed neutron emission from excited states of ^{17}O, which are formed following the 4.17-s half-life β^- decay of ^{17}N [34]. The ^{17}N is produced by the $^{18}O(\gamma,p)$ reaction in the sample. Further details are presented in Ref. [20], which reports the $^{18}O((\gamma,pn)+(\gamma,d))$ cross section.
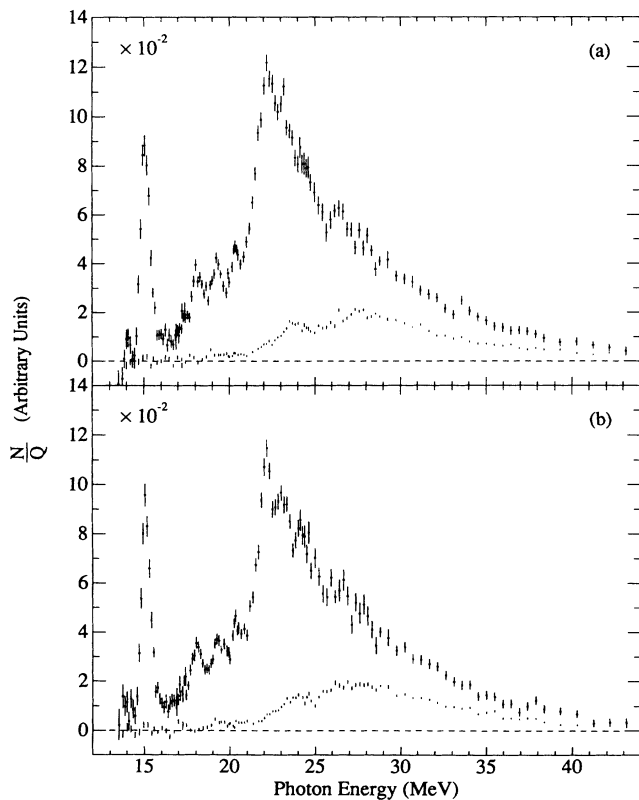

FIG. 3. Comparison of the yields from the H_2^{17}O (upper data points) and H_2^{18}O (lower data points) samples due to annihilation photons only, obtained from (a) the 27.94 cm×13.97 cm NaI and (b) the 20.32 cm×20.32 cm NaI.

The cross section σ at each photon energy was calculated from the expression

$$\sigma = \left[\frac{N}{Q}\right]_w^{net} \frac{Q}{A}(SAF)\frac{1}{\varepsilon} \ . \qquad (3)$$

Here $(N/Q)_w^{net}$ is the weighted (by the inverse square of the error bars) average of the net yields from the two detectors given by Eq. (2). The net yield from the 20.32 cm×20.32 cm NaI spectrometer was normalized prior to averaging to that from the 27.94 cm×13.97 cm NaI spectrometer by multiplying by a constant factor of 1.06. This factor was determined from the ratio of the two yields taken at all energies and simply reflects the difference in the relative efficiencies of the two detectors. The absolute photoproton efficiency for detecting photoproton events ε was then given by the photopeak efficiency, determined only for the 27.94 cm×13.97 cm NaI as outlined in Sec. II B, multiplied by (i) the ratio of counts in the photopeak to that in the summation region 5.2–7.1 MeV (determined from spectra taken with the sample to an accuracy of better than ±1%) and (ii) 0.67, being the number of 6.13-MeV γ rays per reaction [34].

In Eq. (3), Q/A is the number of photon-flux monitor units per annihilation photon, which increases linearly with energy; the calibration used in this measurement was determined in Refs. [26] and [28]. The solid-angle factor SAF is a constant correction to the value of Q/A resulting from the method used in the calibration. It takes into account the difference in the solid angles subtended at the annihilation target by the NaI detector used in the calibration [26,28] and by the collimator used to define the beam striking the sample. It also takes into account the effective number of sample nuclei per unit area that are irradiated.

The resulting cross section is shown in Fig. 4.

B. Experimental uncertainties

The error bars on the individual data points of Fig. 4 represent the statistical uncertainties only. An energy-independent systematic uncertainty of ±8% arises from the determination of the total detection efficiency. The significant contributions in this arise from uncertainties in (i) the absolute number of 6.13-MeV γ rays emitted from the ^{238}Pu-α-^{13}C source (±6%) [35], (ii) the extraction of the photopeak area from the 6.13-MeV γ-ray spectra recorded from the ^{238}Pu-α-^{13}C source (±5%), and (iii) the branching ratio for β^- decay of ^{16}N leading to emission of 6.13-MeV γ rays (±1%) [34].

The significant energy-dependent systematic uncertainties are the following: (i) The uncertainty in Q/A increases in a near-linear way, from ±3% at $E_\gamma \simeq 12$ MeV to ±9% at $E_\gamma \simeq 42$ MeV [26]. (ii) The uncertainty in the photon-flux normalization constant k of ±1.5% [26] translates into an uncertainty in the absolute cross section of $\lesssim 1\%$ for $E_\gamma \lesssim 24$ MeV and ~8% at $E_\gamma = 30$ MeV. Above $E_\gamma = 30$ MeV the positron bremsstrahlung contribution to the measured photoproton yield dominates more and more, as seen in Fig. 2. This increases the uncertainty in the cross section to ~25% at $E_\gamma = 35$

MeV and ~55% at $E_\gamma = 40$ MeV. (iii) Distortions in some energy regions of the cross section of up to about ± 30 μb might be introduced by the interpolation and smoothing of the yields as mentioned above; the effect on

structure in the cross section is expected to be minimal.

The overall systematic uncertainty in the cross section was estimated by summing the above components in quadrature. This uncertainty is $\pm 10\%$ at $E_\gamma \lesssim 26.5$ MeV
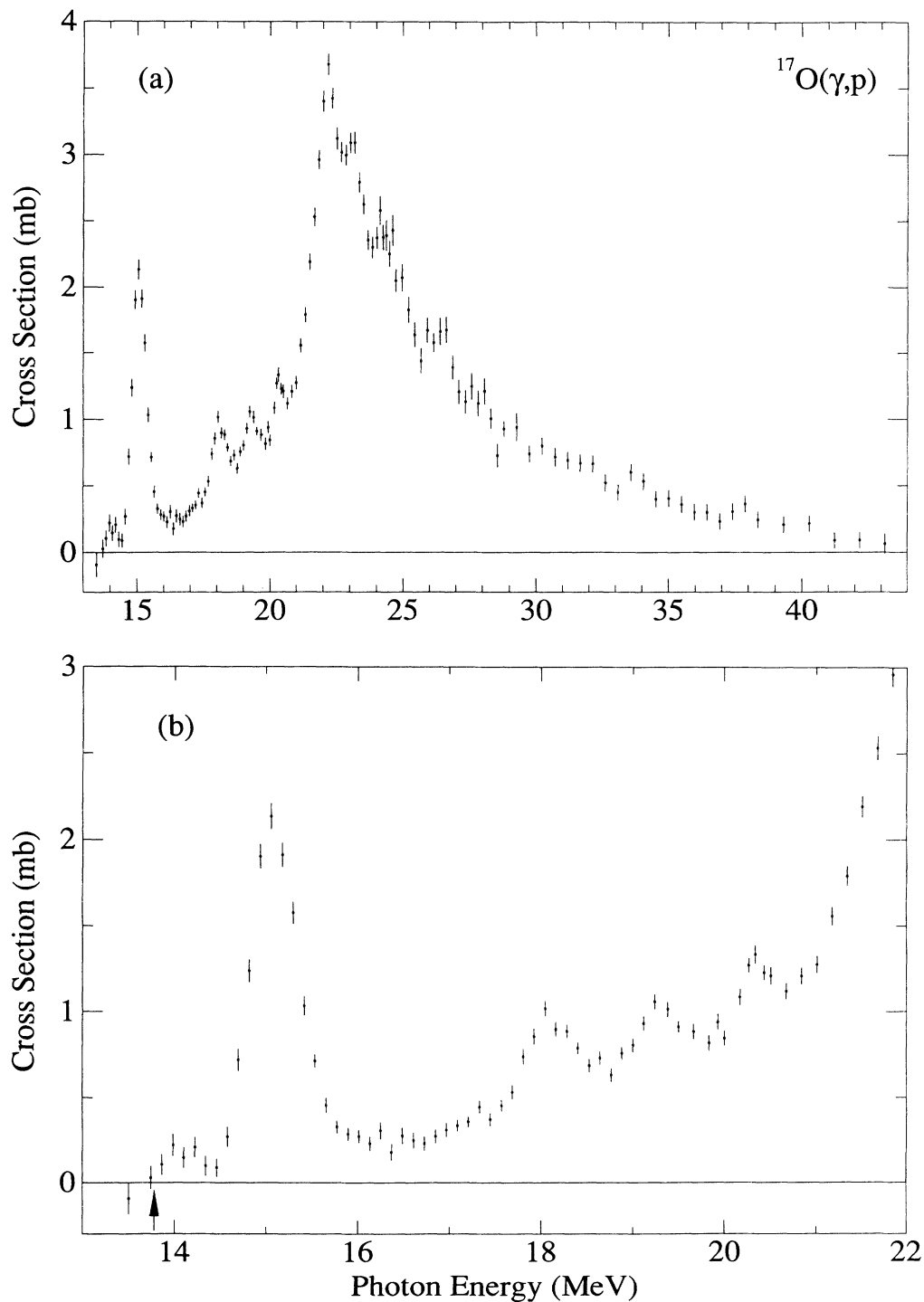

FIG. 4. ^{17}O$(\gamma,p)^{16}$N reaction cross section. Part (a) shows the cross section over the entire range of the measurement, and part (b) gives more detail of the region below the GDR. The error bars indicate the statistical uncertainties only. The arrow in part (b) indicates the reaction threshold at 13.78 MeV.

and increases almost linearly to $\pm \sim 18\%$ at $E_\gamma \simeq 33$ MeV, followed by a further almost linear increase to $\pm \sim 75\%$ at $E_\gamma \simeq 43$ MeV.

IV. RESULTS

A. Cross section

Figure 4(a) shows the ^{17}O(γ,p) reaction cross section measured from 13.50 MeV (just below the 13.78-MeV threshold) to 43.15 MeV. The cross section is observed to have a significant amount of structure, characteristic of the photoproton cross sections of other light nuclei. The main strength, clearly forming part of the ^{17}O GDR, is concentrated in the region from 21 to 26 MeV and is centered at ~ 23 MeV, with a width of ~ 5.5 MeV. In this GDR region, clear peaks are observed at 22.2, 23.1, and 24.4 MeV and a less well-defined peak at ~ 26.5 MeV. The maximum cross section observed is 3.68 ± 0.08 mb at 22.17 MeV, which is somewhat smaller than the magnitudes of photoproton cross sections of other light nuclei. Above 27 MeV the cross section tails off to near zero at ~ 44 MeV. Within the photon-energy resolution of the present experiment, no unambiguous structure is observed above 27 MeV.

Figure 4(b) shows the detail in the cross section below the GDR. A weak peak is observed near threshold, at 14.1 MeV, and a pronounced asymmetric peak at 15.06 MeV. A shoulder is barely evident at 17.1 MeV, and clear peaks in this low-energy region are also observed at 18.1, 19.3, and 20.3 MeV.

To facilitate further discussion and to allow comparison with data from other studies of ^{17}O, the structure in the region 17–21 MeV was fitted with noninterfering modified Lorentz curves. Prior to χ^2 fitting of the data, the Lorentz curves were convoluted with a Gaussian having a width chosen to match the photon-energy resolution near the resonance energies. The positions and widths of the peaks (assumed to be single resonances) determined in this way are listed in Table II. The uncer-

tainties in the widths of these resonances result mainly from the uncertainties in estimating the underlying contribution from the GDR. The effect of this contribution on the derived widths was estimated by assuming different shapes for the rising tail of the main GDR strength. This procedure has a minimal effect on the peak positions, and hence the uncertainties associated with the peak energies are smaller.

It should be noted that the measured cross section shown in Fig. 4 represents decays by emission of single protons from ^{17}O leading to the population of the ground state $(J^\pi = 2^-)$ of ^{16}N and the low-lying excited states at 120 keV (0^-), 297 keV (3^-), and 397.5 keV (1^-) only. These states are shown in Fig. 5, together with the relevant kinematic data for ^{17}O photoreactions. All other excited states in ^{16}N that can be populated are unbound; the (γ, pn) threshold is at 16.27 MeV (2.49 MeV in excitation for ^{16}N). Since the probability of gamma decay from unbound states relative to particle decay is lower, typically by several orders of magnitude, then essentially all ^{17}O(γ,p) events leading to states in ^{16}N higher in excita-

TABLE II. Peaks observed in the ^{17}O$(\gamma,p)^{16}$N cross section.

Photon energy[a] (MeV)	Width (MeV)
(14.1 $\pm$0.1)[b]	
15.06$\pm$0.05	$\sim$0.45[c]
((17.1 $\pm$0.1))[b]	
18.09$\pm$0.07[d]	0.59$\pm$0.14
19.28$\pm$0.07[d]	0.75$\pm$0.20
20.33$\pm$0.07[d]	0.30$\pm$0.10
22.17$\pm$0.1	$\sim$1
23.1 $\pm$0.1	
24.4 $\pm$0.1	
(26.5 $\pm$0.15)[b]	

[a]Uncertainty in the energy calibration is about $\pm$0.25%.
[b]Parentheses indicate peaks that are not well established.
[c]Estimated from the observed width of $\sim$625 keV and experimental energy resolution of $\sim$320 keV using the procedure given in Ref. [38].
[d]Uncertainty includes $\pm$20 keV from the fit discussed in the text.
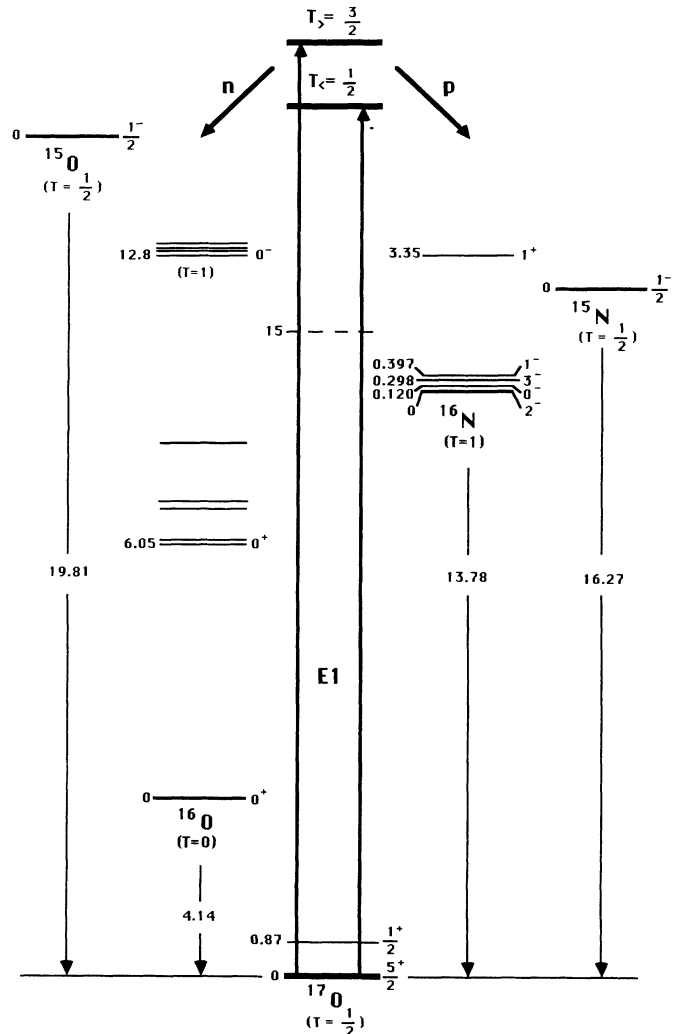

FIG. 5. Kinematic data for the ^{17}O photoreactions. Some of the relevant nuclear levels are shown. All energies are given in MeV.

tion energy than 2.49 MeV will result in the subsequent emission of a neutron (or a proton if above 15.27 MeV in ^{16}N). Contributions from reactions where neutrons are emitted in association with protons, such as (γ,pn) and (γ,np), are included in the ^{17}O(γ,sn) cross section of Jury *et al.* [1].

B. Integrated cross section

The integrated cross section for the ^{17}O$(\gamma,p)^{16}$N reaction from threshold (13.78 MeV) to 43.15 MeV, the upper limit of the present measurement, is 26.7 ± 3.7 MeV mb. This exhausts 10.6% of the Thomas-Reiche-Kuhn (TRK) sum rule. The integral up to 30 MeV is 21.9 ± 2.3 MeV mb and up to 40 MeV is 26.3 ± 3.4 MeV mb. The quoted uncertainties include only systematic uncertainties in the cross section; the statistical uncertainties make an insignificant contribution.

C. Estimate of the ^{17}O(γ,tot) cross section

The (γ,tot) cross section for ^{17}O can be approximated by summing the present (γ,p) cross section and the (γ,sn) cross section of Jury *et al.* [1], where

$$\sigma(\gamma,sn)=\sigma(\gamma,n)+\sigma(\gamma,np+pn)+\sigma(\gamma,2n)+\sigma(\gamma,n\alpha)$$
$$+\sigma(\gamma,3n)+\cdots . \qquad (4)$$

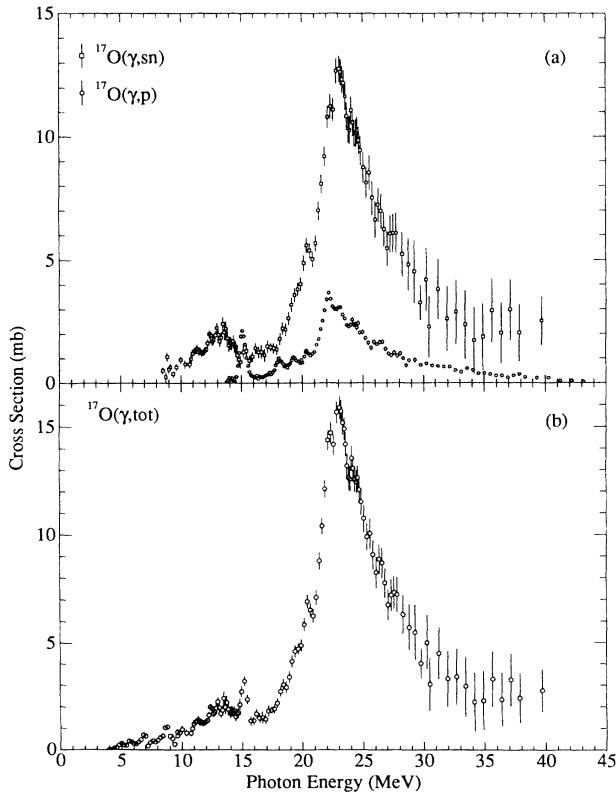FIG. 6. (a) ^{17}O$(\gamma,p)^{16}$N cross section reported here compared with that for ^{17}O(γ,sn) reported by Jury *et al.* [1]. (b) ^{17}O(γ,tot) cross section, obtained by summing the cross sections shown in part (a) and also including the preliminary ^{17}O(γ,n) cross-section data of Eden, Thompson, and Zubanov [39] below 10 MeV.

Included below 10 MeV is the preliminary (γ,n) data measured at Melbourne [39]. The (γ,p) and (γ,sn) cross sections, shown in Fig. 6(a), were both measured at LLNL with similar annihilation-photon resolution and energy calibration, thereby minimizing distortions in taking their sum. It should be noted that the absolute cross-section scales are nearly independent since different detectors and photon-flux monitors were used; these are the major source of systematic uncertainties. Since the (γ,sn) cross section is larger than the (γ,p) by a factor of ~4, the uncertainty in the (γ,tot) cross section stems mainly from the (γ,sn) cross section, which was estimated in Ref. [1] to vary from 7% below 20 MeV to somewhat less than 20% at the highest energies measured.

Indications from neighboring nuclei are that reactions such as the (γ,α), (γ,d), $(\gamma,^3\text{He})$, etc., contribute less than a few percent to the (γ,tot) strength [2]. For ^{17}O, only the contributions from the $(\gamma,^3\text{H}_0)$ and $(\gamma,^3\text{He}_0)$ reactions are available [34]. The capture cross section for the ^{14}N$(^3\text{H},\gamma_0)^{17}$O [7] and the ^{14}C$(^3\text{He},\gamma_0)^{17}$O [6] reactions result, after detailed balancing, in maximum photonuclear cross sections of only ~45 μb (near 21 MeV) and ~200 μb (in the GDR), respectively. We do not expect the sum of contributions from such reactions to exceed several percent of the ^{17}O(γ,tot) strength shown in Fig. 6(b).

V. DISCUSSION

A. Photoproton reaction

As noted above, the (γ,p) cross section reported here results from population of the ground state of ^{16}N (2^-) and the first three low-lying excited states at 120 keV (0^-), 297 keV (3^-), and 397.5 keV (1^-) only. These final states are known to have very pure 1p-1h nature. Shell-model calculations incorporating a full p-s-d shell basis [3] predict $>96\%$ $(1p_{1/2})^{-1}(1d_{5/2})^1$ configuration for the 2^- and 3^- states and $>98\%$ $(1p_{1/2})^{-1}(2s_{1/2})^1$ configuration for the 0^- and 1^- states. Thus the proton decay of 2p-1h configurations with $(1p_{1/2})^{-1}$ components is represented, while the decay both of 2p-1h configurations with $(1p_{3/2})^{-1}$ components and of more complex configurations (3p-2h, 4p-3h, etc.) formed from the correlated ^{17}O ground state will be suppressed because of their insignificant parentage involving a proton coupled to the ^{16}N final states. The proton decay of configurations with $(1p_{3/2})^{-1}$ components will populate the unbound levels of ^{16}N, the strength of which is represented in the (γ,pn) reaction and included in the $(\gamma,1n)$ cross section [1].

This selectivity is valid only for (γ,p) strength produced via the semidirect process. The dominance of the semidirect process in the (γ,p) reaction has been established recently by O'Rielly, Zubanov, and Thompson [5] in a measurement of the deexcitation γ rays emitted in the ^{17}O$(\gamma,p\gamma')^{16}$N reaction. About 10% of the proton decays populate the 0^- and 1^- states in ^{16}N, which is a measure of the nonsemidirect processes (i.e., preequilibrium and statistical), since the 0^- and 1^- states have a

$(\nu 2s_{1/2})^1$ configuration and thus can only be reached from the $(\nu 1d_{5/2})^1$ ground state of ^{17}O if scattering occurs. Assuming that the nonsemidirect strengths for 2^- and 3^- states are comparable to the 0^- and 1^- states, we see that $\sim 80\%$ of the (γ,p) strength results from the semidirect process. The study of the proton pickup reaction ^{17}O($d,^3$He)^{16}N by Mairle et al. [40] confirms the strong population of the 2^- and 3^- states; they see no population of the 0^- and 1^- states. Furthermore, all of the observed spectroscopic strength from the $1p_{1/2}$ subshell is carried by the 2^- and 3^- states. On this basis, the (γ,p) cross section represents all of the proton-transition strength from the $1p_{1/2}$ subshell.

A comparison of the (γ,p), (γ,sn), and (γ,tot) cross sections is made in Fig. 6. In the main GDR region, the (γ,p) cross section is only $\sim 20\%$ of the (γ,tot) cross section, which can be taken as evidence of the dominance of $(1p_{3/2})^{-1}$ components in the wave function of the strong $E1$ states of ^{17}O. The ratio $\sigma(\gamma,\text{tot})/\sigma(\gamma,p)$ increases with excitation energy, which indicates an increase in the relative importance of $(1p_{3/2})^{-1}$ components as one passes through the GDR. There is no major restructuring of cross-section strength from $(1p_{1/2})^{-1}$ and $(1p_{3/2})^{-1}$ components. The splitting in energy of strength from transitions $1p_{1/2} \rightarrow 2s\text{-}1d$ and $1p_{3/2} \rightarrow 2s\text{-}1d$ can be estimated from the center of strength in the (γ,p) and (γ,sn) cross sections. We exclude the (γ,n) strength in the pygmy resonance, since it originates from transitions $1d_{5/2} \rightarrow 1f\text{-}2p$ (see below), and we assume that the energy distribution of the transitions $\nu 1p_{1/2} \rightarrow 2s\text{-}1d$ and $\pi 1p_{1/2} \rightarrow 2s\text{-}1d$ are the same. A separation of ~ 1.6 MeV is obtained, which represents a measure of the configurational splitting within the $1p$ shell.

A large fraction of the total photoproton strength for ^{17}O, corresponding to the transitions from the $1p_{3/2}$ subshell, is represented in the (γ,pn) reaction. Since the photoproton reaction mechanism is dominated by the semidirect process, the (γ,pn) and (γ,p) integrated strengths should be proportional [4] to the summed spectroscopic factors for the unbound and bound levels of ^{16}N, respectively (i.e., a factor of ~ 1.5 [40]). We estimate that the (γ,pn) integrated strength is comparable to the (γ,p) strength reported here, after allowing for the lower penetrabilities of the (γ,pn) channels. Further support for the large (γ,pn) strength comes from the following observations.

(i) The measured average neutron energy in the $(\gamma,1n)$ reaction is low (~ 3.5 MeV) and constant in the GDR region ($E_\gamma \approx 19\text{--}27$ MeV) [1], indicating strong population of the high-lying states in ^{16}O and ^{16}N, which become even stronger with increasing excitation energy.

(ii) The observation of strength (~ 0.6 mb above ~ 24 MeV) in the $(\gamma,2n)$ cross section [1] is significant, since it might indicate population of $T=1$ states in ^{16}O above 15.67 MeV from $T=\frac{3}{2}$ states in the GDR of ^{17}O (see Fig. 5). The $(\gamma,np+pn)$ channels (which open at 16.27 MeV) compete strongly with the $(\gamma,2n)$ channels (which open at 19.81 MeV), as is suggested by the slow rise in the $(\gamma,2n)$ cross section extending for a few MeV above threshold (see Fig. 3 of Ref. [1]).

(iii) In the GDR region, the (γ,sn) cross section is a factor of ~ 4 larger than the (γ,p). A factor of 2 is expected on the basis of Clebsch-Gordan coefficients coupling the $T=\frac{3}{2}$ states in ^{17}O (which are dominant in the GDR region) and the $T=1$ analogs of ^{16}O and ^{16}N. The factor of ~ 4 may be understood if strength comparable to that observed in the (γ,p) reaction reported here is carried by the unbounded ^{16}N states, consistent with expectations based on proton pickup data.

(iv) At energies above the GDR, the $(\gamma,1n)$ cross section [which includes the $(\gamma,np+pn)$ strength] is ~ 2.5 mb. Assuming that the (γ,n) cross section tails off in the same way as the (γ,p), then the $(\gamma,np+pn)$ channels carry most of the (γ,tot) strength in this region.

It is noteworthy that around 40 MeV single-proton emission from ^{17}O contributes very little to the (γ,tot) strength, which is consistent with the expected [41] onset near this energy of the quasideuteron mechanism of photon absorption leading to emission of correlated proton-neutron pairs.

B. Structure in the cross section

To facilitate the discussion of structure observed in the present cross section, Fig. 7 summarizes the relevant photonuclear-reaction data.

1. 14.1-MeV peak

A weak but clear peak is observed at 14.1 MeV, only 320 keV above threshold. It is significant that it is seen, despite the size of the Coulomb barrier, which severely suppresses decays by proton emission. If a $T_<$ state at this energy were photoexcited, it would decay so strongly by neutron emission that the proton channels would not be seen. However, if it were a $T_>$ state, neutron decay would be isospin forbidden to the low-lying $T=0$ states of ^{16}O, leaving the proton channels, despite the low penetrability, as the only available decay mode. It is thus highly probable that this peak in the ^{17}O(γ,p) cross section indicates a $T=\frac{3}{2}$ state in ^{17}O at 14.1 MeV.

A state in ^{17}O has been reported [34] at 14.15 ± 0.10 MeV, with a width of about 100 keV. Its tentative J^π assignment is $\frac{9}{2}^+$ or $\frac{11}{2}^+$, with no isospin assignment. Because the J^π assignment is tentative, identification of this state with that seen in the present experiment cannot be ruled out. Also, the state observed in this experiment might be the analog of a $J^\pi;T=\frac{3}{2}^-;\frac{3}{2}$ state in the mirror nucleus ^{17}F at 14.176 MeV with a width of 30 ± 5 keV [34].

In the photoneutron cross section [1], a shoulder can be seen near this energy, suggesting that this state might be isospin admixed. If this were the case, evidence of it should be seen in other particle-decay channels [for example, the (γ,α)]. A strong resonance near this energy should be manifest in photon-scattering measurements.

2. Pronounced resonance near 15 MeV

The (γ,p) cross section shows a pronounced resonance located at 15.06 MeV, just 1.3 MeV above the photopro-

ton reaction threshold. Despite a Coulomb barrier of ~ 2 MeV, the resonance is remarkably strong relative to the main GDR peak at 22.2 MeV and exhausts about 6% of the cross section integrated over the entire energy range covered in the present measurement. The resonance has a clear asymmetry; the half width at half maximum on the high-energy side of the peak is a factor of 1.3 greater than that at the low-energy side. Even after taking into account the strength from the GDR tail, it falls more slowly on the high-energy side. It is possible that the asymmetry is due to barrier-penetrability effects: The Coulomb barrier suppresses proton emission to a greater extent on the low-energy than on the high-energy side. However, the observed asymmetry also could result from the excitation of more than one state
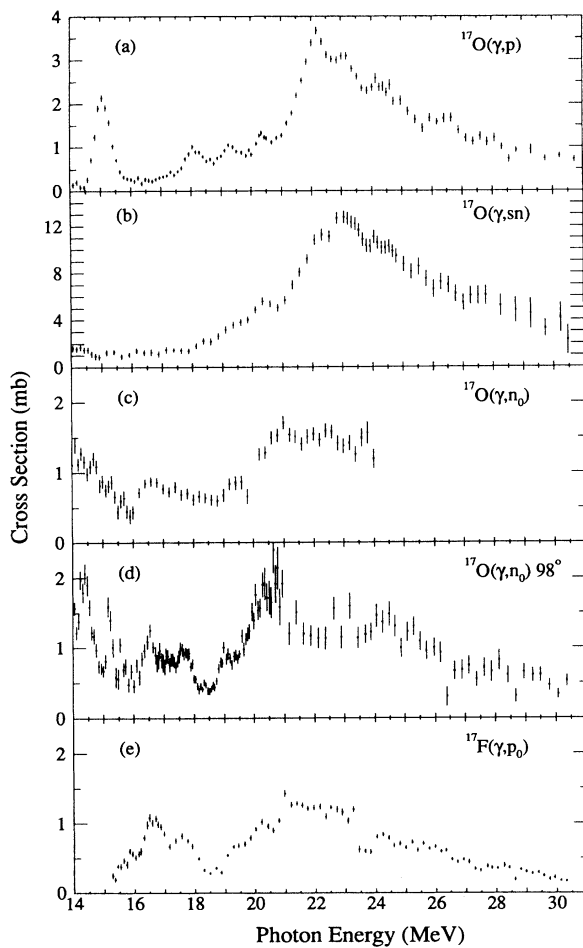
Proton emission to the low-lying states of ^{16}N (which have $T=1$) can occur from both $T=\frac{1}{2}$ and $\frac{3}{2}$ states in ^{17}O. However, neutron decay from $T=\frac{3}{2}$ states in ^{17}O to $T=0$ states in ^{16}O is isospin forbidden. Neutron decay from $T=\frac{3}{2}$ states in ^{17}O becomes allowed at an energy of 16.94 MeV (in ^{17}O), when decay to the first $T=1$ state in ^{16}O (at 12.80 MeV) becomes energetically possible. Thus, below 16.94 MeV, $T=\frac{3}{2}$ states in ^{17}O are forbidden to decay by neutron emission, while neutron decay of $T=\frac{1}{2}$ states is allowed—and favored by penetrabilities—to any of the many available $T=0$ states in ^{16}O. Figure 8 shows the available photoneutron data for ^{17}O near 15 MeV. The absence of a strong resonance both in the (γ,sn) cross section [1] and in the integrated-over-angles (γ,n_0) cross section [12]—which, in good isospin, selects only $T=\frac{1}{2}$ strength—provides strong evidence for an isospin assignment of $T=\frac{3}{2}$ for the major part of the strength in this peak.

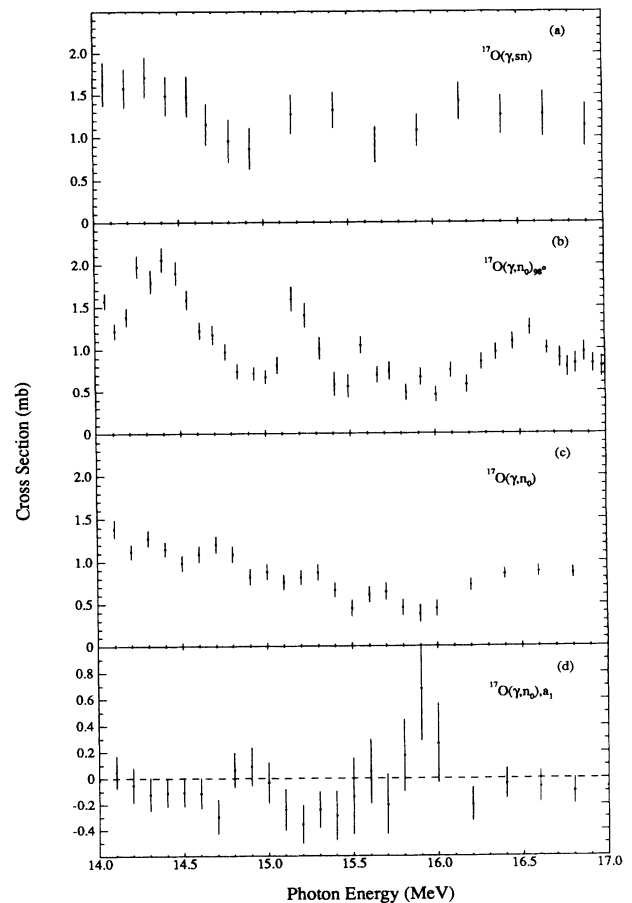The FWHM of this peak at 15.06 MeV is 625 ± 50 keV. After correcting for the experimental resolution of ~ 320

FIG. 7. Comparison of the photonuclear data for mass 17: (a) the $^{17}O(\gamma,p)$ cross section (present data), (b) the $^{17}O(\gamma,sn)$ cross section of Jury *et al.* [1], (c) the $^{17}O(\gamma,n_0)^{16}O$ integrated-over-angles cross section of Jury *et al.* [12], (d) the $^{17}O(\gamma,n_0)^{16}O$ 98°-differential cross section of Johnson *et al.* [11] multiplied by 4π and energy corrected according to Ref. [50], and (e) the $^{17}F(\gamma,p_0)^{16}O$ cross section obtained using detailed balance from the $^{16}O(p,\gamma)^{17}F$ 90°-excitation function measured by Harakeh, Paul, and Gorodetzky [14] and which was normalized to an integrated cross section of 10.2 MeV mb estimated in Ref. [14] from angular distributions measured at a few energies.

FIG. 8. Comparison of the available photonuclear data for ^{17}O around 15 MeV: (a) the (γ,n) cross section of Jury *et al.* [1]; (b) the (γ,n_0) 98°-differential cross section of Johnson *et al.* [11], multiplied by 4π and energy corrected according to Ref. [50]; (c) the integrated-over-angles (γ,n_0) cross section $(4\pi A_0)$ of Jury *et al.* [12], and (d) the Legendre coefficient a_1 for the (γ,n_0) reaction [12].

keV [30], the width becomes ~450 keV. Hinterberger et al. [42] have studied the $T=\frac{3}{2}$ states in ^{17}O by measuring the neutron transmission on ^{16}O and find it probable that $T=\frac{3}{2}$ states in the 14–16-MeV region have widths that are characteristically 50 keV or less. In this energy range, the width of a $T=\frac{3}{2}$ state results almost entirely from the proton channels; all other open particle channels [(γ,n), (γ,α), and (γ,d)] are isospin forbidden [34]. The total widths of $T=\frac{3}{2}$ states in this energy region are expected to be narrow because of the small number of open (γ,p) channels and the low penetrability of those channels. The observation of a peak whose width is an order of magnitude larger than the characteristic width strongly suggests that more than one state is contributing.

That more than one level may be photoexcited near 15 MeV is indicated by the observation of two peaks in the ^{17}O(e,e') spectra measured at 75° by Norum, Bergstrom, and Caplan [15]. One is at 14.76 MeV (> 300 keV wide) and another stronger peak is seen at 15.24 MeV (~200 keV wide). Unfortunately, the quality of the electron-scattering data in this energy region was not good enough to determine the transition multipolarities [15]. There is also a pronounced structure at ~15.2 MeV in the (γ,n_0) reaction (see below).

Because this resonance is strong, $E1$ transitions are expected to contribute. Several narrow levels have been reported in the 14.5–15.5-MeV region of excitation in ^{17}O [34]. The properties of most of these levels are not fully established, and the corresponding levels in the mirror ^{17}F nucleus are even less well known [34]. Although a few of the reported levels may be $E1$ accessible, none has an established assignment of $J^\pi = \frac{3}{2}^-$, $\frac{5}{2}^-$, or $\frac{7}{2}^-$, required for an $E1$ transition from the $\frac{5}{2}^+$ ground state of ^{17}O.

At energies just above 15.06 MeV—the peak of the resonance—two possible non-$E1$ levels are reported [34], which, if photoexcited, may account for the observed asymmetry in the peak. Both were observed by Hinterberger et al. [42] in their high-resolution study of the ^{16}O$+n$ reaction. One was observed at 15.198 MeV with $\Gamma = 52\pm14$ keV and the other at 15.37 MeV with $\Gamma = 40\pm6$ keV. If analog association is made between these two states and those at 4.01 and 4.21 MeV in ^{17}N, then J^π assignments of $\frac{3}{2}^+$ and $\frac{7}{2}^+$ are determined for the 15.198- and 15.37-MeV levels, respectively. The analog association of the 15.198-MeV level in ^{17}O with the 4.01-MeV level in ^{17}N has been confirmed by Cunsolo et al. [43] in a parallel investigation of the ^{14}C$(^6$Li,^{3}H$)^{17}$O and ^{14}C$(^6$Li,^{3}He$)^{17}$N reactions. Hinterberger et al. [42] have been able to observe these levels because of their nonzero isospin-forbidden neutron-decay widths; the ground-state neutron decay widths Γ_{n_0} for the 15.198- and 15.37-MeV levels are ~10% (5.5 keV) and ~5% (~2 keV) of the total width, respectively. Since the widths Γ_{n_0} are small but significant, evidence for photoexcitation of these levels should be sought in the (γ,n_0) reaction.

A pronounced peak is observed at ~15.2 MeV in the ^{17}O(γ,n_0) 98°-differential cross section of Johnson et al.

[11], shown in Fig. 8(b), which is confirmed by the 90° data of Jury et al. [12]. There is little evidence of structure in this energy region in the integrated-over-angles ^{17}O(γ,n_0) cross section of Jury et al. [12], shown in Fig. 8(c), consistent with the small Γ_{n_0} found [42] for both levels. Furthermore, the asymmetry Legendre coefficient a_1 from the fitted angular distributions [see Fig. 8(d)] changes from a value of ~0 at 15.0 MeV to ~ −0.35 in the region from 15.1 to 15.5 MeV, indicating $E1$-$M1$ (or $E2$) interference. Thus there is evidence for the photoexcitation of at least one of the two positive-parity levels (at 15.198 and 15.37 MeV). We expect these levels to be observed in photoproton channels since these channels provide the only isospin-allowed mode for particle decay. The asymmetry observed on the high-energy side of the peak probably represents strength from these levels.

Levels with J^π of $\frac{3}{2}^+$ and $\frac{7}{2}^+$ are accessible from the $\frac{5}{2}^+$ ground state of ^{17}O via $M1$ or $E2$ transitions. We prefer $M1$ transitions, since the $M1$ giant resonance is expected to be located in light nuclei at an excitation energy of $\sim 35A^{-1/3}$ MeV [44], which, for ^{17}O, is at ~13.6 MeV. The isovector $E2$ strength, on the other hand, is believed [44] to be centered at $\sim 130A^{-1/3}$ MeV (i.e., ~50 MeV for ^{17}O). We may have located the major part of the giant $M1$ resonance in ^{17}O; the strength in the asymmetry component (~0.03 mb) exhausts a large fraction of the Gell-Mann–Telegdi sum rule for $M1$ transitions [45] (0.05 mb for ^{17}O). The inverse energy-weighted strength for the 15-MeV resonance is 0.10±0.01 mb, which is twice that given by the $M1$ sum rule [45]. Thus, as noted earlier, it is unlikely that all of the strength in this resonance corresponds to pure $M1$ transitions. It is noteworthy that the angular distributions for the (γ,n_0) reaction on the low-energy side of the resonance ($\lesssim 15.0$ MeV) are consistent with $E1$ excitation.

Only one report of $M1$ transitions has been made in ^{17}O, at 15.10 MeV, that by Rangacharyulu et al. [46] in their high-resolution (e,e') study at 153° (measured from 11 to 15.3 MeV). This state was so weakly excited [$B(M1) \sim 0.1\mu_N^2$] that photoexcitation would contribute only ~0.1 MeV mb to the 15-MeV resonance, and so is unlikely to account for the asymmetry in the 15-MeV resonance and for the structure observed in the (γ,n_0) reaction. On the basis of the narrow width of this level, it was concluded that it did not correspond to the 15.198-MeV $\frac{3}{2}^+$ state seen in the ^{16}O$+n$ study [42]. Interestingly, in their published spectrum (see Fig. 2 of Ref. [46]), a wider peak is observed at 15.20 MeV, but no comments were made regarding its excitation mode.

The existence of $M1$ transitions in ^{17}O indicates that ground-state correlations of the ^{16}O core are present in this nucleus. Strong correlations of the ^{16}O core are expected, since significant $M1$ strength has been found in both ^{16,18}O nuclei [47]. However, to date, very little $M1$ strength has been found in ^{17}O. The present work indicates that additional $M1$ strength in ^{17}O may be found in a $\frac{3}{2}^+$ level at 15.198 MeV and also possibly a $\frac{7}{2}^+$ level at 15.37 MeV. Clearly, this region should be explored further with the (e,e') reaction at large backward angles in order to confirm the present arguments and determine

the $M1$ transition strength of any such levels for comparison with $M1$ strength found in ^{16,18}O [47].

3. 18.1-MeV peak

There is no evidence of a resonance at 18.1 MeV either in the ^{17}O$(\gamma, n_0)^{16}$O integrated-over-angles cross section of Jury et al. [12] or in the ^{17}O$(\gamma, n_0)^{16}$O 98°-differential cross section of Johnson et al. [11]. However, it should be noted that the absence of a resonance in the $T_<$-selective ^{17}O$(\gamma, n_0)^{16}$O reaction does not necessarily imply that the observed structure must have $T = \frac{3}{2}$, since the configuration of this state might be such that there is no parentage involving a neutron coupled to the ground state of ^{16}O. Nonetheless, the fact that there is no evidence of a resonance at this energy in the ^{17}O(γ, sn) cross section [1] implies that no significant population of $(T=0)$ excited states in ^{16}O occurs and weighs the argument further in favor of a $T = \frac{3}{2}$ assignment. Consistent with this assignment is the absence of a peak near 18.1 MeV in the $T_<$-selective ^{16}O$(p, \gamma)^{17}$F reaction [14].

However, the 590-keV width of the peak observed in the present measurement seems too large for a $T = \frac{3}{2}$ level near 18 MeV. The total width of $T = \frac{3}{2}$ levels in the region from 14 to 16 MeV is characteristically small, $\lesssim 50$ keV [42,34]: This width comes about almost entirely because of the availability of the isospin-allowed proton-decay channels to $T=1$ states in ^{16}N, which open at 13.78 MeV. For a $T = \frac{3}{2}$ level in ^{17}O near 18 MeV, the number of isospin-allowed decay channels has doubled as a result of the opening of the neutron-decay channels to $T=1$ states in ^{16}O, which open at 16.94 MeV. (The opening of the ^{15}N$+n+p$ decay channels at 16.27 MeV has a minimal effect.) With the number of channels effectively doubled and an increase in the penetrabilities for the ^{16}N$(T=1)+p$ channels, the width of $T = \frac{3}{2}$ levels near 18 MeV may increase by a factor of roughly 2–3; an order-of-magnitude increase would be unusual. Thus, on the basis of its width, it would seem that this peak has $T = \frac{1}{2}$. Furthermore, this 18.1-MeV peak is comparable in width to those seen in this experiment at 19.3 and 20.3 MeV, for which a $T = \frac{1}{2}$ assignment is argued below.

Since no levels of width comparable to that observed in this experiment are reported in ^{17}O near 18 MeV, the possibility that this broad peak in the ^{17}O$(\gamma, p)^{16}$N cross section might be the result of two or more states should be considered. Two states are listed in the Ajzenberg-Selove compilation [34] around 18 MeV, only one of which can be photoexcited by $E1$ radiation: that at 18.110 MeV with $J^\pi; T = \frac{3}{2}^-; \frac{3}{2}$ and $\Gamma = 46 \pm 12$ keV. A small ground-state neutron-decay width (~ 1.0 keV) has been determined for this level, which is consistent with the absence of strength at 18.1 MeV in the (γ, n_0) cross section [11,12]. If this state were excited in the present measurements, its narrow width of 46 keV could not alone account for the observed width.

Evidence from photoneutron data [1,11] exists for photoexcitation of a level at about 18.3 MeV, which together with the 46-keV-wide level mentioned above, can account

for the 590-keV width of this peak. In the ^{17}O(γ, sn) cross section [1], a clear shoulder is observed at ~ 19.3 MeV, which corresponds to the 19.3-MeV resonance in the present ^{17}O$(\gamma, p)^{16}$N cross section. If strength with the characteristics of this resonance is removed from the ^{17}O(γ, sn) cross section, the presence of a level at about 18.3 MeV is revealed. Further evidence of this level is available from the ^{17}O$(\gamma, n_0)^{16}$O 98°-differential cross section of Johnson et al. [11] shown in Fig. 7(d), where a clear bump is observed at about 18.3 MeV. No clear indications of a resonance are seen in the lower-resolution ^{17}O$(\gamma, n_0)^{16}$O integrated-over-angles cross section of Jury et al. [12], although the possibility of weak strength cannot be discarded.

Although a state in ^{17}O at 18.3 MeV is not included in the Ajzenberg-Selove compilation [34] or any analog state been reported at the appropriate energy in ^{17}F, there is evidence from the photonuclear data for its existence. Furthermore, in a study of the ^{13}C$(^6$Li$,d)^{17}$O$^* \rightarrow \alpha + ^{13}C_{g.s}$ reaction measured by Cardella et al. [18], a strong peak was observed in the deuteron-energy spectrum at an energy corresponding to an excitation of 18.3 MeV; the same state has been observed earlier in the same reaction by Artemov et al. [49]. Assuming good isospin, α decay to the $T = \frac{1}{2}$ ground state of ^{13}C must come from a $T = \frac{1}{2}$ state in ^{17}O, an assignment consistent with the observation of the 18.3-MeV state in the ^{17}O$(\gamma, n_0)^{16}$O reaction.

In summary, the peak observed at 18.1 MeV is probably a doublet consisting of (i) a $T = \frac{3}{2}$ level corresponding to that reported [42,34] at 18.101 MeV with $J^\pi = \frac{3}{2}^-$ and a width of 46 keV, and (ii) a $T = \frac{1}{2}$ level at 18.3 MeV, which is weakly excited in the (γ, n_0) reaction, has preference for decaying to excited states in ^{16}O and which may have an α-cluster structure. (It should be noted that the available data for the second level also are consistent with it being an isosopin-admixed $T_>$ state which can decay by ground-state neutrons and alphas through its $T_<$ component.)

4. 19.28-MeV resonance

The presence of a peak at 19.3 MeV in the ^{17}O(γ, n_0) integrated-over-angles cross section [12] with a width similar to that observed in this experiment at 19.28 MeV dictates an isospin assignment of $T = \frac{1}{2}$ for this state in ^{17}O. The ^{17}O$(\gamma, n_0)^{16}$O 98°-differential cross section measured by Johnson et al. [11] also shows a clear peak at 19.2 MeV. In view of the estimated ± 100-keV uncertainty at these energies in the modified energy scale [50] of the work of Johnson et al., there is little doubt that this peak is caused by the same level as that observed in the present experiment and that of Jury et al. [12]. At this energy there is clear evidence as well for a shoulder in the ^{17}O(γ, sn) cross section [1]. The strength in this shoulder is too large to be accounted for by ground-state neutrons only; most of the neutron decays are to the excited states in ^{16}O. Also, the $T = \frac{1}{2}$ analog in the mirror ^{17}F is observed as a clear shoulder at ~ 19.4 MeV in the ^{17}F$(\gamma, p_0)^{16}$O cross section [14] shown in Fig. 7(e).

This $T = \frac{1}{2}$ level in ^{17}O can be identified with the resonance which appears to be present at $\sim$19.3 MeV in the 90°-excitation function for the $T_<$-selective reaction ^{14}N(^{3}H,$\gamma_{0,1}$)^{17}O, reported by Linck, Kraus, and Blatt [7]. Additional evidence for this resonance is available in the mirror reaction ^{14}N(^{3}He,γ_{0+1})^{17}F reported by Mo, Blue, and Weller [51]; an $\sim$300-keV-wide resonance was observed at 19.42$\pm$0.05 MeV and most likely corresponds to the shoulder evident at $\sim$19.4 MeV in the ^{17}F(γ,p_0)^{16}O cross section [14]. Following ^{3}H capture by ^{14}N, transitions to both the $\frac{5}{2}^+$ ground state (γ_0) and $\frac{1}{2}^+$ first excited state (γ_1) at 0.87 MeV in ^{17}O appear to resonate at this level [7]. Assuming dipole-only transitions, the spins of resonances seen in the γ_0 excitation function are limited to $J = \frac{3}{2}, \frac{5}{2}$, or $\frac{7}{2}$, while those in the γ_1 channels are limited to $J = \frac{1}{2}$ or $\frac{3}{2}$; observation in both reactions implies $J = \frac{3}{2}$. The strength of this resonance in the ^{17}O(γ,p)^{16}N and ^{17}O(γ,sn) cross sections and the dominance of $E1$ radiation in photonuclear cross sections favors negative parity. The value of the asymmetry Legendre coefficient a_1 of $\sim$0 near 19.3 MeV observed in the ^{17}O(γ,n_0)^{16}O reaction [12] further supports the $E1$ assignment.

The decay of this dipole state via the (γ,p), (γ,sn), (γ,n_0), and ($\gamma,^3$H$_0$) reaction channels suggests a mixed-configuration structure. The present (γ,p) cross section selects predominantly 2p-1h components. It is reasonable to suppose that ^{3}H emission is proportional to the 3p-2h components of the continuum wave function [8]. Comparison of the integrated cross sections over the resonance in these reactions can give an indication of the relative importance of the two components. The resonance strength in the ($\gamma,^3$H$_0$) reaction, obtained from the inverse capture reaction using the principle of detailed balance, is roughly 0.5% of the (γ,p) strength. However, penetrabilities favor the emission of $l=2$ protons over $l=0$ tritons by around a factor of 500; any other l values increase this factor. Hence the reduced ($\gamma,^3$H$_0$) strength is considerably larger than the (γ,p) strength. It appears that 3p-2h components are more important than 2p-1h in the description of this dipole state.

Furthermore, a state has been reported at 19.3 MeV in the ^{13}C(^{6}Li,d)^{17}O*$\rightarrow\alpha+^{13}$C$_{g.s.}$ reaction by Artemov et al. [49] and, more recently, by Cardella et al. [48], who studied the same reaction and observed a strong state at 19.4 MeV. Because the peak in the deuteron spectrum is superimposed on a steep continuum, the excited state occurs at a lower energy, closer to 19.3 MeV (see Fig. 1 of Ref. [48]). Assuming good isospin, this reaction favors $T = \frac{1}{2}$ states. This state probably corresponds with the structure observed in the photonuclear reactions, indicating that α-cluster components might also be present in the wave function of this dipole state.

5. 20.33-MeV resonance

A clear peak, of about the same width as that observed in the present measurement, is seen in the ^{17}O(γ,sn) cross section [1] at 20.3 MeV. The ^{17}O(γ,n_0) 98°-differential cross section of Johnson et al. [11] shows a strong peak

at 20.3 MeV, comparable in width to that reported here. Therefore, the most probable isospin assignment for this structure is $T = \frac{1}{2}$. This peak is not evident in the ^{17}O(γ,n_0) measurement of Jury et al. [12], but poor resolution would preclude its being seen there. Further support for this isospin assignment is available in the ^{17}F(γ,p_0)^{16}O reaction [14], where the $T = \frac{1}{2}$ mirror analog state is evident as a clear peak at 20.2 MeV. This state might also correspond to that observed at 20.4 MeV in the ^{16}O(n,n)^{16}O reaction [52], which excites only $T = \frac{1}{2}$ resonances in ^{17}O; $\Gamma_n/\Gamma \simeq 0.7$ was estimated, which is consistent with the strength observed in the ^{17}O(γ,sn) cross section relative to that in the total absorption cross section.

The 20.33-MeV resonance can be identified with that observed at 20.39$\pm$0.05 MeV with $J^\pi = \frac{5}{2}^\pm$ or $\frac{7}{2}^-$ and $\Gamma = 660\pm70$ keV by Linck, Kraus, and Blatt [7] in the $T_<$-selective ^{14}N(^{3}H,$\gamma_{0,1}$)^{17}O reaction. An $E1$ transition is favored since a strong resonance is observed in the ^{17}O(γ,p)^{16}N and ^{17}O(γ,sn) cross sections. Therefore, the $J^\pi = \frac{5}{2}^+$ assignment can be discarded. Furthermore, in the mirror reaction ^{14}N(^{3}He,γ_{0+1})^{17}F, Mo, Blue, and Weller [51] reported an $\sim$350-keV-wide resonance at 20.25$\pm$0.05 MeV with $J^\pi = \frac{7}{2}^-$, which probably corresponds to the 20.2-MeV resonance evident in the ^{17}F(γ,p_0) reaction [14]. This $T = \frac{1}{2}$ state in ^{17}F is very likely to be the mirror analog of the level observed in ^{17}O. If this association is correct, then an assignment of $J^\pi = \frac{7}{2}^-$ can be made.

The integrated cross section over this resonance in the ($\gamma,^3$H$_0$) reaction, obtained from the inverse capture reaction using the principle of detailed balance, is smaller than that in the (γ,p) reaction by about a factor of 10. Linck, Kraus, and Blatt [7] report that their 20.39-MeV resonance is formed by capture of $l=3$ tritons. Penetrabilities hinder $l=3$ triton emission with respect to proton ($l>0$) by more than a factor of 1000. Hence the reduced ($\gamma,^3$H$_0$) strength is larger than the (γ,p) by at least two orders of magnitude. It is reasonable to assume that triton emission is directly related to the 3p-2h component of the continuum wave function [8]. Therefore, it appears that the amplitude of 3p-2h configurations in the wave function of this resonant state is dominant and that the neglect of these configurations in any calculation of dipole states near 20 MeV in ^{17}O is not justified.

6. Structure in the GDR region

The intermediate structures observed clearly in the (γ,p) cross section at 22.2, 23.1, and 24.4 MeV are seen as well in the (γ,sn) cross section [1]. The weak structure evident in the (γ,p) cross section as a dip at 25.5 MeV and a peak at $\sim$26.5 MeV is not seen in the (γ,sn) cross section and is reported here for the first time. Large statistical errors could have masked any evidence for this structure in the (γ,sn) cross section.

Most of the resonance strength in the GDR region is $T_>$; this is supported by the much larger overall strength observed in the photoneutron channels than in the photoproton channels. Furthermore, the peaks at 22 and 23

MeV are both absent from the $T_<$-selective (γ,n_0) reaction [11,12] so that a $T=\frac{3}{2}$ assignment for both peaks is therefore preferred, but is not guaranteed. The structure at 24.4 MeV is indicated in the (γ,n_0) reaction [11], suggesting a $T=\frac{1}{2}$ assignment. This assignment may be considered tenuous, since $T_>$ states in the GDR region are generally more isospin admixed and therefore can decay via the isospin-forbidden channels through their $T_<$ components.

Two major differences in the (γ,p) and (γ,sn) cross sections are observed in the GDR region: the 22.2-MeV peak, dominating the (γ,p) cross section, is less pronounced in the (γ,sn) cross section—the dominant structure in that cross section occurs at 23 MeV; and the broad shoulder observed in the (γ,sn) cross section at ~ 28 MeV is not seen in the (γ,p) cross section. These differences cannot be attributed to changes in the isospin nature of the major structures, but could arise from changes in the configuration of $E1$ states as one passes through the GDR. The selectivity of the (γ,p) reaction to $(1p_{1/2})^{-1}$ components and the (γ,sn) to mainly $(1p_{3/2})^{-1}$, discussed in Sec. V A, suggests that the change in relative strength of the two peaks reflects a relative enhancement of $(1p_{3/2})^{-1}$ components at 23 MeV, which become more dominant in the configurations of $E1$ states at ~ 28 MeV.

Importance of 3p-2h configurations.—Table III summarizes the known resonances in ^{17}O in the energy region of the GDR. The resonances observed in the radiative capture reaction ^{14}C(^{3}He,γ)^{17}O measured by Chang, Diener, and Ventura [6] are particularly interesting, since this reaction probes the 3p-2h components of the continuum wave function [8]. If the reduced strengths of resonances seen in the $(\gamma,^3$He$_0)$ reaction were significant compared to those observed for (γ,p) reaction—which probes 2p-1h states only—then there would be a good reason to consider 3p-2h configurations in the theoretical treatment of core-excited states in ^{17}O.

The $E1$-accessible resonance $(J^\pi=\frac{7}{2}^-)$ observed at

22.1 ± 0.1 MeV ($\Gamma\sim750$ keV) in the $(^3$He,$\gamma_0)$ reaction [6] may be identified with that observed in the present work at 22.2 MeV ($\Gamma\sim1$ MeV). The resonance observed at 24.4 MeV in the $(^3$He,$\gamma_1)$ excitation function may correspond to that seen in the present work at the same energy; if correspondence is made, then the resonance has $J^\pi=\frac{3}{2}^-$, since the $(^3$He,$\gamma_1)$ reaction selects $J^\pi=(\frac{1}{2},\frac{3}{2})^-$ states (the first excited state in ^{17}O has $J^\pi=\frac{1}{2}^+$) and the photonuclear reactions select $J^\pi=(\frac{3}{2},\frac{5}{2},\frac{7}{2})^-$. The positive-parity levels observed in the $(^3$He, $\gamma_1)$ are excited mainly via $E2$ transitions [6] and are not likely to contribute significant strength in the photonuclear reaction.

We can estimate the importance of 3p-2h components near 22 MeV. At 22.2 MeV the (γ,p) cross section is 3.7 mb, while the on-resonance $(\gamma,^3$He$_0)$ cross section obtained from the $(^3$He,$\gamma_0)$ cross section by detailed balance is 0.21 mb. Making a correction for the different penetrabilities of ^{3}He particles and protons, on the basis of 8-MeV (outgoing) protons ($l=2$) and 4.1-MeV ^{3}He particles ($l=3$ [6]), leads to a $(\gamma,^3$He$_0)$ reduced strength that is about 30% of the (γ,p). This suggests that 3p-2h components play a significant role in the GDR, at least for the resonance at 22.2 MeV. Brown and Green [55] have indicated the presence of significant admixtures of the type $(1p_{1/2})^{-2}(1d_{5/2})^3$ in the ground state of ^{17}O, so that the 3p-2h negative-parity states evidenced in the ^{3}He-capture reaction could be formed by $E1$ excitation from this $1d_{5/2}$ admixture. The $\frac{7}{2}^-$ state at 22.2 MeV may then be a combination of 2p-1h and 3p-2h configurations, with the former dominating.

C. Integrated cross-section systematics for ^{12,13,14}C, ^{14,15}N, and ^{16,17,18}O

The photoproton and photoneutron cross sections, integrated up to 30 MeV, for the entire series of measurements encompassing ^{12,13,14}C, ^{14,15}N, and ^{16,17,18}O are given in Table IV. The ^{12}C, ^{14}N, and ^{16}O values are from an evaluation by Fuller [2]; the other values have been

TABLE III. Resonances observed in the GDR region of ^{17}O.

(γ,p)[a] (MeV)	(γ,sn)[b] (MeV)	(γ,n_0)[c] (MeV)	(e,e')[d] (MeV)	Other[e] E_x (MeV)	J^π	Γ (keV)
				21.7[f,g]	$\frac{5}{2}^+$	~750
22.2	22.2		22	22.1[f,g,h,i]	$\frac{7}{2}^-$	~750
				22.5[f]	$\frac{3}{2}^{(-)}$	~1000
				23.0[f,g]	$\frac{1}{2}^+$	~400
23.1	23		23			
				23.5[f]		
24.4	24.4	24.4[j]		24.4[f]		
		(25.1)				
(26.5)						
	~28[k]					

[a]Present work.
[b]Reference [1].
[c]References [11] and [12].
[d]Reference [15].
[e]Reference [34].
[f]Reference [6].

[g]Reference [53].
[h]Reference [54].
[i]Reference [49].
[j]Also evident in the ^{16}O(p,γ)^{17}F reaction [14].
[k]Broad shoulder.

updated from papers forming part of this systematic study. The photoneutron cross sections for this C-N-O series are complete, while the present measurement, together with the recently published measurement of the ^{14}C(γ,p) cross section [24], completes the photoproton series.

On the basis of the weak-coupling model [10], the (γ,sn) strength is expected to increase as each extra neutron is added to a closed $4n$ core. For the $A = 4n$, $4n+1$, and $4n+2$ systems, experimental evidence strongly supports this expectation. The ^{16,17,18}O nuclei display a systematic increase in photoneutron strength of around 0.15 TRK sum-rule unit up to 30 MeV, as detailed in Table IV. The photoneutron strength for the ^{12,13,14}C series also increases, but in a less systematic way (a large increase followed by a smaller increase), probably because the doubly magic oxygen core is more closed than the filled $1p_{3/2}$-subshell carbon core. Similar trends are also apparent in the ^{24,25,26}Mg and ^{28,29,30}Si systems (see Ref. [60]). Interestingly, the photoneutron strength for ^{28,29,30}Si nuclei also increases systematically by around 0.15 TRK unit, whereas the ^{24,25,26}Mg series displays relative changes in photoneutron strength similar to those for ^{12,13,14}C. These systematics suggest that the degree of closure of the ^{16}O core is similar to that of the ^{28}Si core and that of ^{12}C is similar to that of ^{24}Mg, the two former

being more closed than the two latter. It should also be noted that the addition of a proton hole followed by a neutron hole to the ^{16}O core (the ^{15,14}N systems) again systematically increases the photoneutron strength by around 0.15 TRK unit.

Using this simple picture, the integrated photoproton cross section is expected to drop systematically in order to maintain an essentially constant $E1$ absorption strength. This trend is seen in ^{16,18}O, ^{14,15}N, and ^{12,13,14}C. However, the present photoproton cross section introduces a deviation from this trend. The drop in strength between ^{16,17}O is about a factor of 2 larger than the expected drop of 0.15 TRK unit. This lower photoproton strength for ^{17}O relative to that for ^{16,18}O might be due to a substantially larger (γ,pn) strengths for this nucleus; the (γ,pn) strength is carried by the (γ,sn) cross section. The (γ,pn) $[+(\gamma,np)]$ strength for ^{16,18}O (up to 30 MeV) are small [0.013 (see Ref. [2]) and 0.023 (Ref. [20]) TRK unit, respectively]. The discussion in Sec. V A supports a value for the ^{17}O(γ,pn) strength comparable to that for (γ,p), i.e., roughly 0.1 TRK unit. When this correction is made to the value in Table IV for ^{17}O, the expected systematic decrease in the total photoproton strength for the oxygen isotopes becomes apparent. However, the total photoabsorption cross section for ^{17}O, taken to be the sum of the photoneutron and photoproton integrated

TABLE IV. Integrated photonuclear cross sections for ^{12,13,14}C, ^{14,15}N, and ^{16,17,18}O.

Nucleus	E_γ^{max} (MeV)	S_n^a (MeV)	$\int_{S_n}^{E_\gamma^{max}} \sigma(\gamma,sn)dE_\gamma$ (MeV mb)	(TRK)^c	S_p^a (MeV)	$\int_{S_p}^{E_\gamma^{max}} \sigma(\gamma,p)dE_\gamma$ (MeV mb)	(TRK)^c	Sum^b (TRK)^c
^{12}C	30	18.72	43.1^d	0.241^d	15.96	71.6^{d,e}	0.400	0.641
^{13}C	30	4.95	95.5^f	0.495	17.53	42^g	0.218	0.712
^{14}C	30	8.18	108^h	0.527	20.83	17^i	0.083	0.610
^{14}N	30	10.55	113.0^d	0.540	7.55	25.2^d	0.121	0.661
^{15}N	30	10.83	92^j	0.412	10.21	52^k	0.233	0.646
^{16}O	30	15.66	57.6^d	0.241^d	12.13	105.0^{d,e}	0.439	0.680
^{17}O	30	4.14	97.5^l	0.385	13.78	21.9^m	0.087	0.472
^{18}O	30	8.04	142.5^n	0.537	15.94	30.7^n	0.116	0.652
^{16}O	40	15.66	80.7^d	0.338	12.13	125^{d,o}	0.523	0.861
^{17}O	40	4.14	123^{l,p}	0.486	13.78	26.3^m	0.104	0.590
^{18}O	40	8.04	192^n	0.723	15.94	43.2^n	0.163	0.886

^{a}Separation energies are taken from Ref. [37].

^{b}Uncertainty is ± 10–15 %.

^{c}Thomas-Reiche-Kuhn sum-rule units, $59.74NZ/A$.

^{d}From an evaluation by Fuller [2] of the available photonuclear-reaction data.

^{e}Value given is the $\sigma(\gamma,sp)=\sigma(\gamma,p)+\sigma(\gamma,2p)+\sigma(\gamma,p\alpha)+\sigma(\gamma,3p)+\cdots$, but not $\sigma(\gamma,pn)$, which is included in the $\sigma(\gamma,sn)$.

^{f}Reference [33].

^{g}Reference [56] (extrapolated from 28 MeV).

^{h}Reference [32].

^{i}Reference [24].

^{j}Reference [57] (below 26.5 MeV) and Ref. [58] (above 26.5 MeV).

^{k}Sum of partial cross sections for population of the ground and the 7.01-MeV states in ^{14}C, the only states populated following single-proton emission in the measurement reported in Ref. [59].

^{l}Reference [1] (above 10 MeV) and preliminary (γ,n) cross-section data from Ref. [39] (below 10 MeV).

^{m}Present work.

^{n}Reference [29].

^{o}Estimated from values in Table 4.4 of Ref. [2].

^{p}Data from Ref. [1] was extrapolated from 39.7 MeV.

cross sections up to 30 MeV, also exhausts significantly less than the expected $\frac{2}{3}$ TRK unit, the fraction exhausted by its neighbors.

In order to see if the $^{17}O(\gamma,tot)$ integrated cross section that appears to be missing is to be found above 30 MeV (the limit of integration used above), the summation limit was extended to 40 MeV for $^{16,17,18}O$, and these data also are included in Table IV. The trends are observed to be the same as in the region below 30 MeV, with the total absorption strength for ^{17}O now being lower by about 0.3 TRK unit, compared to both ^{16}O and ^{18}O. Reactions such as (γ,α), (γ,d), $(\gamma,{}^3He)$, etc., each contribute typically less than 2% to the integral of the total cross section to 30 MeV for ^{12}C, ^{14}N, and ^{16}O [2] and are expected to be of similar significance for their non-self-conjugate neighbors. For example, the $^{14}N(^3H,\gamma_0)^{17}O$ [7] and $^{14}C(^3He,\gamma_0)^{17}O$ [6] radiative capture cross sections, when converted by detailed balance to the inverse photonuclear cross sections, give, respectively, 0.054 MeV mb (integrated to 21.3 MeV) and 0.49 MeV mb (integrated to 24.9 MeV); their sum thus contributes less than 1% to the integrated (γ,tot) cross section. If the lower total absorption strength for ^{17}O relative to its neighbors cannot be accounted for by these small-component reactions, the missing dipole strength might be found above 40 MeV.

The total photonuclear cross section integrated up to the meson threshold ($\sim$140 MeV) is given by the Levinger-Bethe sum rule [61] as $60NZ(1+\kappa)/A$ MeV mb, where the factor κ is usually interpreted as a measure of the two-body meson exchange currents. For ^{16}O, $(1+\kappa)=1.40$ ($\pm10\%$) [62], and κ is expected [63] to decrease by only a few percent for ^{17}O as the neutron excess and mass increase. If one expects that the integrated cross section for ^{17}O up to 140 MeV also exhausts near 1.40 TRK units, then the ^{17}O strength in the region 40–140 MeV would need to exceed that for ^{16}O by about a factor of 1.6.

At higher energies the photonuclear reaction mechanism is dominated by the (γ,pn) process in which the photon is absorbed by a correlated neutron-proton pair (the quasideuteron effect) [41,61]. Therefore, any large increase in the $^{17}O(\gamma,tot)$ cross section above 40 MeV might be an indication of a much large quasideuteron contribution than is present in ^{16}O. Such a situation is not likely, since the critical parameters in Levinger's model [61], namely, the number of p-n pairs and Levinger factor (L), are not expected to change significantly from ^{16}O to ^{17}O. It is, therefore, not expected that the major part of the strength that appears to be missing below 40 MeV is to be found in the 40–140-MeV region.

The relatively low (γ,tot) strength for ^{17}O remains unexplained. It is noteworthy that the magnitude of the present measurement has been confirmed in the recent measurement of the $^{17}O(\gamma,p\gamma')^{16}N$ reaction by O'Rielly, Zubanov, and Thompson [5].

D. Comparison of the $^{16,17,18}O(\gamma,p)$ cross sections

Figure 9 shows the $^{16,17,18}O(\gamma,p)$ cross sections. The ^{16}O photoproton cross section is the $^{16}O(\gamma,sp)$ cross section obtained by Fuller [2], and the $^{18}O(\gamma,p)^{17}N$ cross section is that published by Woodworth et al. [29].

These cross sections reflect almost entirely transitions from the $1p$ shell. Differences in shapes of these cross sections must therefore be a measure of the effect of the valence neutrons on the doubly magic ^{16}O core. The intermediate structure observed in the $^{17,18}O(\gamma,p)$ cross section is also reflected in the $^{17,18}O(\gamma,sn)$ cross sections, but is less pronounced. The $^{17,18}O(\gamma,p)$ reactions, having thresholds (at 13.78 and 15.94 MeV, respectively) which are much higher than those for the $^{17,18}O(\gamma,sn)$ reactions (4.14 and 8.04 MeV), carry cross-section strength from fewer reaction channels than is carried by the $^{17,18}O(\gamma,sn)$ cross sections. In addition, the main GDR structure observed in the $^{17,18}O(\gamma,sn)$ cross sections, resulting mainly from core excitations, is obscured to some extent by strength arising from the valence neutrons. Core effects are therefore more noticeable in the photoproton cross sections.

The $^{16,17}O(\gamma,p)$ cross sections show strikingly similar intermediate structure. Resonances are observed in both near 22.2, 23.1, and 24.4 MeV. The shoulder observed at 25 MeV in the $^{16}O(\gamma,p)$ cross section is not clearly evident in the $^{17}O(\gamma,p)$ cross section; however, it is evidenced in the $^{17}O(\gamma,n_0)$ 98°-differential cross section of Johnson et al. [11] [see Fig. 7(d)]. This strong similarity indicates that the valence neutron only weakly perturbs the ^{16}O core, so that the $E1$ transitions by protons to form the GDR are essentially unchanged in ^{17}O com-
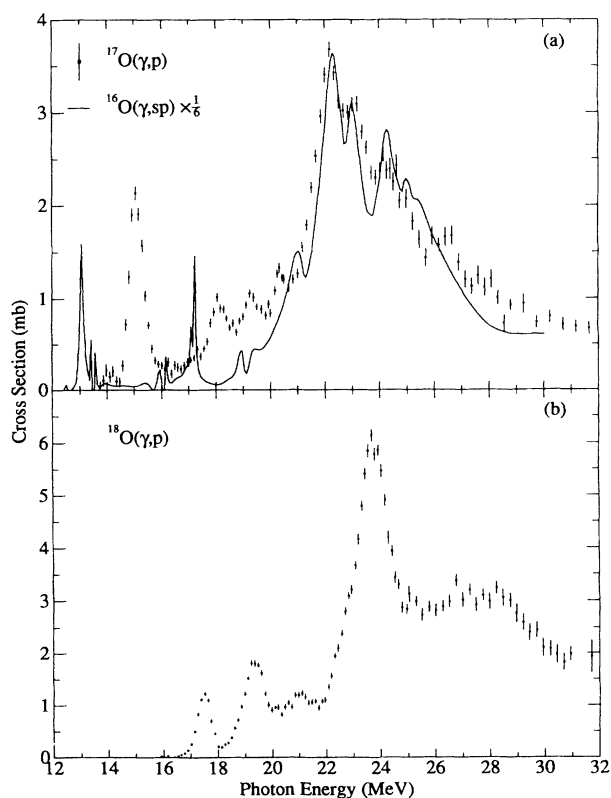
FIG. 9. Comparison of the photoproton cross sections for the oxygen isotopes: (a) the present $^{17}O(\gamma,p)^{16}N$ cross section compared with the $^{16}O(\gamma,sp)$ cross section of Fuller [2] multiplied by $\frac{1}{6}$ and (b) the $^{18}O(\gamma,p)^{17}N$ cross section of Woodworth et al. [29].

pared with those in ^{16}O. This is as expected from the weak-coupling model [10]. The loose binding of this valence neutron is reflected, for example, in the very low ^{17}O(γ,n) threshold (4.14 MeV) and the large rms charge radius of the $1d_{5/2}$ orbit in ^{17}O. This was determined by Hicks [64] from magnetic electron-scattering data to be 3.56 fm, which is larger than the orbit radius of other $1d_{5/2}$ nuclei (e.g., 3.25 fm for ^{25}Mg and 3.40 fm for ^{27}Al). Also, the magnetic dipole moment of ^{17}O is very close to the Schmidt limit.

In contrast, the ^{16}O core is considerably perturbed by the addition of two neutrons. The GDR region of the ^{18}O(γ,p) cross section is dominated by two broad and pronounced structures at 23.7 and 27.5 MeV instead of the four narrower and more tightly clustered peaks observed in the ^{16,17}O(γ,p) cross sections. In the case of ^{18}O, it appears that, far from being spectators which leave the $E1$ transitions of the core essentially unaffected, as is the case for ^{17}O, the two neutrons strongly influence the structure in the GDR [65].

The trends in the ^{16,17,18}O(γ,p) cross sections may be correlated with changes in the ground-state properties related to static deformation, viz., ground-state correlations and rms charge radii. A measure of the correlations of the ^{16}O core in the ground state of the oxygen isotopes is provided by the proton-occupation numbers for the $2s$-$1d$ shell, which were obtained by Mairle et $al.$ [66] by summing the spectroscopic factors determined from proton pickup data leading to positive-parity excited states in the residual nuclei. The proton occupation numbers for the $2s$-$1d$ shell of 0.45, 0.29, and 0.94 are reported for ^{16,17,18}O, respectively. A similar trend is obtained from shell-model calculations, [67] viz., 0.35, 0.32, and 0.83 for ^{16,17,18}O, respectively. These numbers may be interpreted to arise from changes in deformation of the core [66,68]. The large increase in the proton-occupation probability for the $2s$-$1d$ shell from ^{16,17}O to ^{18}O is consistent with the known deformation-parameter values for ^{16}O $(\beta = -0.084)$ and ^{18}O $(\beta = -0.35)$ [4].

It is interesting to note that similar trends are followed by the charge radii. The rms charge radii of ^{16,17,18}O have been determined [69] by elastic electron scattering; the result obtained is $R_{17} < R_{16} < R_{18}$ and the radii are in ratio R_{16}:R_{17}:$R_{18} = 1.000$:0.995 ± 0.006:1.020 ± 0.005. Both the proton-occupation numbers for the $2s$-$1d$ shell and the charge radii indicate that a single neutron perturbs the ^{16}O core minimally (if anything, it is slightly tightened), whereas a pair of neutrons significantly alters the core.

We observe that the changes in $E1$ core excitations between ^{16}O and ^{17}O are minimal and the changes between ^{16,17}O and ^{18}O are major, consistent with the above trends. It appears that a pair of neutrons in ^{18}O, in deforming the already deformed ^{16}O core, causes a major redistribution of $E1$ strength from the core, whereas the single neutron in ^{17}O, in having essentially no effect on the core, also causes a minimal change in $E1$ transitions from the core. The large observed shift in energy of resonances in ^{18}O is therefore not surprising. Also, the larger number of valence protons in the $2s$-$1d$ shell for ^{18}O results in Pauli blocking of proton excitations from the ^{16}O

core and so might account for the suppression of some of the weaker transitions observed in ^{16,17}O to produce a less-structured ^{18}O(γ,p) cross section in the GDR region. In addition, the distribution of valence protons among the three $2s$-$1d$ subshells caused by deformation might also account for differences in structure and relative strength observed below the GDR in the ^{16,17,18}O(γ,p) cross sections.

A similar situation exists in the carbon isotopes [24,70]. The $1p_{1/2}$-subshell proton-occupation numbers for ^{12,13,14}C show that the addition of $1p_{1/2}$ neutrons leads to a consolidation of the $1p_{3/2}$ proton subshell closure. The number of protons in the $1p_{1/2}$ subshell decreases from 0.7 in ^{12}C to about 0.4 in ^{13}C and to 0.3 in ^{14}C [68]. This decrease was interpreted by Mairle and Wagner [68] to result from decreasing nuclear deformation (from about $\beta = -0.3$ to -0.1) as a function of increasing neutron number. The photonuclear cross sections for the carbon isotopes show some redistribution of $E1$ strength and an increase in the GDR position, from ~ 23 MeV for ^{12}C to ~ 24.5 MeV for ^{13}C and to ~ 25.6 MeV for ^{14}C [2,24,32], which also may be linked with changes in static deformation.

E. ^{16,17}O(γ,p) cross-section structure and the core-excitation model

By appealing to the core-excitation model [71], we can obtain an indication of the strength of the interaction between the core and valence neutron in ^{17}O. According to this model, the $J^{\pi} = 1^{-}$ $(T=1)$ collective (assumed) excited states formed by $E1$ transitions from the ^{16}O core should couple to the valence neutron in its $1d_{5/2}$-ground-state orbital to form the core multiplets $J^{\pi} = \frac{3}{2}^{-}$, $\frac{5}{2}^{-}$, and $\frac{7}{2}^{-}$ $(T = \frac{1}{2}$ or $\frac{3}{2})$. The probability of populating each member of the multiplet is proportional to $2J+1$, and the energy centroid of the multiplets is predicted to coincide with the energy of the core excitation. The magnitude of the energy splitting depends on the strength of the interaction between the core and valence particle, and in the absence of a strong interaction these states will be nearly degenerate.

The close resemblance in structure of the ^{16,17}O(γ,p) cross sections in the GDR region, as noted above, suggests that, if the core-excitation model were valid for ^{17}O (configuration mixing might affect the predictions of the model), the strength of the interaction would be very weak, and consequently the energy separation of the multiplets would be too small for them to be resolved. The resonances in ^{17}O appear to be only slightly broader than their counterparts in ^{16}O, which might result from the formation of the predicted multiplets with a separation of the order of 100 keV or less.

F. Comparison with shell-model calculations

The photoabsorption cross section for mass-17 nuclei has been calculated in the particle-hole shell-model framework by several authors: (i) Albert et $al.$ [16] used both a modified zero-range Soper interaction and a separable Tabakin interaction; (ii) Eden and Assafiri [17] used the Cooper-Eisenberg interaction; and (iii) Harakeh,

Paul, and Gorodetzky [14] used the Kuo-Brown interaction. Negative-parity states were calculated using the Tamm-Dancoff approximation with harmonic-oscillator single-particle wave functions in a basis of good isospin and a pure $1d_{5/2}$ ground state. States with $T = \frac{3}{2}$ were constructed from 2p-1h configurations and $T = \frac{1}{2}$ states were constructed either from 2p-1h configurations only [(ii)] or from both 1p-0h and 2p-1h configurations [(i) and (iii)]. For the 1p-0h configurations, the $1f$-$2p$ shell was active for the particle, and for the 2p-1h configurations, the $2s$-$1d$ shell was accessible to the particle. The entire $1p$ shell was active for the hole. These authors all used the unperturbed single-particle and single-hole energies derived from experimental data by Jolly [72]. The main difference between these calculations is in the form of the residual nucleon-nucleon interaction that was used. It is of interest to see whether the general features of the photoabsorption cross section for ^{17}O are reproduced within the framework of a truncated shell-model basis and also to note which form for the residual interaction, within this truncation, gives best agreement with experiment.

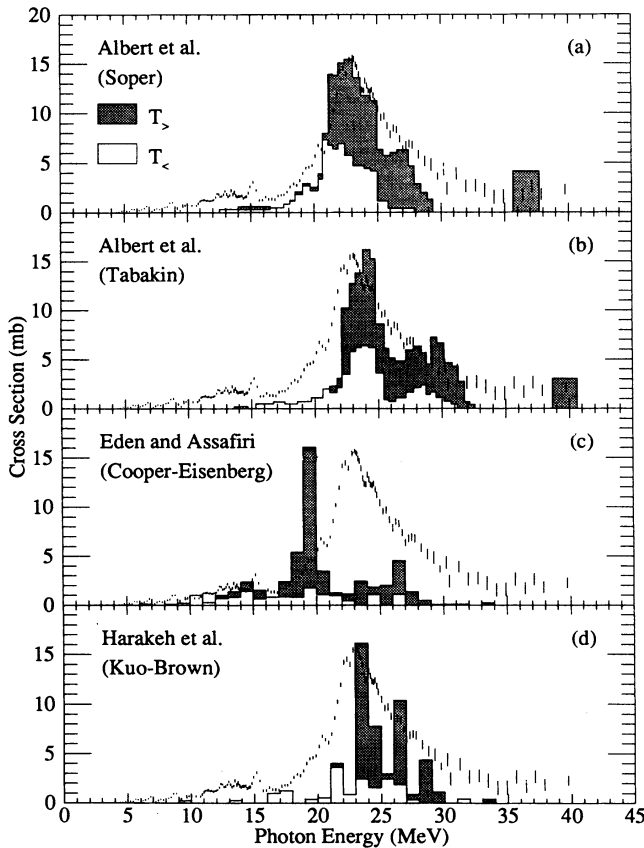The photoabsorption cross section, constructed from

the sum of the (γ,p) and (γ,sn) cross sections, is compared with theoretical calculations in Fig. 10, where the calculated results have been normalized in the GDR region. Albert *et al.* [16] have assigned an arbitrary width of 2 MeV to each predicted level. Eden and Assafiri [17] have summed their dipole strengths in 1-MeV bins. We have calculated the dipole strength for each level predicted by Harakeh, Paul, and Gorodetzky [14] from their tabulated $B(E1)$ values and have summed these in 1-MeV bins.

The predictions using the Soper, Tabakin, and Kuo-Brown residual interactions apportion the main absorption strength into two major peaks. The first and dominant peak forms the main GDR strength and appears at 22–24 MeV, in good agreement with experiment. Roughly one-half of the strength predicted in this peak accounts for the major part of the $T_<$ strength in the GDR. The second, weaker peak, which is mainly $T_>$, is placed 3–5 MeV higher and is evidenced in the present ^{17}O(γ,tot) cross section both as an asymmetry in the GDR which is broader on the higher-energy side and as a weak indication of a dip near 27 MeV [also see the ^{17}O(γ,sn) cross section in Fig. 6].

The calculation of Eden and Assafiri, using the Cooper-Eisenberg interaction, also places the major absorption strength into two groups with relative strengths similar to the predictions using other residual interactions. However, the main GDR component appears about 4 MeV lower than its experimental location. In addition, the larger separation of the two major components of about 7 MeV is not supported by experiment. It seems that this interaction is far better in predicting the distribution of absorption strength for ^{14}C and ^{18}O [32,73] than it is for ^{17}O.

A measure of a part of the $T_<$ distribution in ^{17}O is available from the $T_<$-selective (γ,n_0) cross section [11,12] which accounts for only about 10% of the (γ,tot) cross section in the GDR region. Assuming that the (γ,n_0) reaction faithfully reflects the entire $T_<$ distribution, concentration of $T_>$ strength can then be identified in the three-peak structure centered at ~ 23 MeV and also in the broad shoulder at ~ 28 MeV. The concentration of (γ,n_0) cross-section strength in the region 20–25 MeV and the absence of any major strength at higher energies are consistent with predictions of the $T_<$ distribution.

The three-peak structure apparent in the main peak of the (γ,tot) cross section might correspond to the $T = \frac{3}{2}$ dipole states predicted by Harakeh, Paul, and Gorodetzky [14] at 23.0 ($J^{\pi} = \frac{7}{2}^-$), 23.2 ($\frac{3}{2}^-$), and 24.7 ($\frac{5}{2}^-$) MeV, which dominate the GDR with dipole strengths of 47, 36, and 38 MeV mb, respectively. If the $\frac{7}{2}^-$ state predicted at 23.0 MeV is identified with the resonance observed at 22.2 MeV, which was assigned above as $J^{\pi} = \frac{7}{2}^-$, then the slight displacement in the predicted location could be attributed to the presence in the wave function of the observed resonance of a large 3p-2h component in addition to the dominant 2p-1h component (see above). Also, the extension of basis in the particle-hole calculation to include 3p-2h configurations might frag-

FIG. 10. Comparison between the ^{17}O(γ,tot) cross section $[\sigma(\gamma,\text{tot}) \simeq \sigma(\gamma,p) + \sigma(\gamma,sn)]$ and several theoretical predictions: (a) that of Albert *et al.* [16] using a modified zero-range Soper interaction, (b) that of Albert *et al.* [16] using a Tabakin potential, (c) that of Eden and Assafiri [17] using the Cooper-Eisenberg interaction, and (d) that of Harakeh, Paul, and Gorodetzky [14] using the Kuo-Brown interaction.

ment the strength of this 2p-1h dipole state and bring the relative strengths of the three states into better agreement with experiment.

The Soper and Tabakin potentials predict significant $T = \frac{3}{2}$ strength above 35 MeV, but there is no clear evidence for such strength in the present ^{17}O(γ,p) cross section or in the ^{17}O(γ,tot) cross section. In ^{13}C dipole states have been predicted [16,74] above 30 MeV, which result mainly from the $(1s_{1/2})^{-1}(1p_{1/2})^2$ configuration and for which evidence exists in the ^{13}C(γ,sn) cross section at $\sim$37 MeV [33]. The corresponding structure in ^{17}O is not expected since nucleon transitions from the $1s_{1/2}$ shell to the near-filled $1p$ shell are suppressed by Pauli blocking.

In the present work, $T_>$ strength has been identified in the structure near 15 MeV and in the peak at 18.1 MeV. In the calculations adequate $T_<$ strength to account for this is predicted only using the Soper and the Cooper-Eisenberg interactions. It also seems that the inclusion of isospin and space-exchange terms in the residual interaction (Cooper-Eisenberg) puts more $T_>$ strength in dipole states below the main GDR peak. Eden and Assafiri predict that the $T_>$ strength in the 15-MeV region is concentrated in two states. One is at 14.9 MeV ($J^\pi = \frac{7}{2}^-$) with a strength of 6.1 MeV mb and a dominant (98%) configuration of $(1d_{5/2})^1(2s_{1/2})^1(1p_{1/2})^{-1}$. The other state is at 15.3 MeV ($J^\pi = \frac{5}{2}^-$) with a strength of 5.4 MeV mb and a wave function with the same dominant (92%) $(1d_{5/2})^1(2s_{1/2})^1(1p_{1/2})^{-1}$ configuration plus a small (5%) $(1d_{5/2})^2(1p_{3/2})^{-1}$ component. Both of these states are possible shell-model counterparts for the $E1$ strength in the strong 15-MeV peak.

Also noticeable in the predictions using the Soper, Tabakin, and Kuo-Brown interactions shown in Fig. 10 is the near absence of strength in the region of the observed pygmy resonance. It is argued below that this strength is in fact relocated, and its absence does not reflect a major flaw in these particle-hole shell-model predictions, as has been suggested earlier [1,12].

The single-particle energies for the highly unbound $1f$-$2p$ orbitals used by Harakeh, Paul, and Gorodetzky and Albert et al. greatly affect the predicted strength and location of the pygmy resonance in these calculations. The calculations of Harakeh, Paul, and Gorodetzky are particularly revealing with regard to the origin of the pygmy strength and single-particle energies required to predict its location correctly.

Of the three calculations done by Harakeh, Paul, and Gorodetzky, the one using 2p-1h and 1p basis and the single-particle energies proposed by Jolly [72] predicts the pygmy strength to be due to $1d_{5/2} \rightarrow 1f_{7/2}$ transitions and places the strength between 17 and 18 MeV. This gives the best agreement with strength reported near 17 MeV in their measurement [14] of the ^{16}O(p,γ)^{17}F reaction at 90° [see Fig. 7(e)]; they identified this structure as the pygmy resonance. This identification was not justified in view of the subsequent photoneutron data [1,11,12] for ^{17}O, which has established the location of the pygmy resonance significantly lower, at $\sim$13.5 MeV, with a width of about 4 MeV. Better agreement with ex-

periment would result if the energy of the $1f_{7/2}$ orbital were lowered by $\sim$4 MeV.

The calculations of Harakeh, Paul, and Gorodetzky show that the description of the pygmy resonance requires the inclusion of $1d_{5/2} \rightarrow 1f$-$2p$ single-particle transitions. On the other hand, the calculation of Eden and Assafiri, which ignores the $1f$-$2p$ orbitals, still predicts adequate strength in the region of the pygmy resonance, but this is probably due to the fact that the GDR is located at too low an energy by about 4 MeV, so that the strength in this region is really part of the GDR rather than of the pygmy resonance. The calculations of Albert et al. place very little strength below 17 MeV, the region of the observed pygmy resonance. However, the single-particle energies for the $1f$-$2p$ shell are too high, as discussed above, so that the $1d_{5/2} \rightarrow 1f$-$2p$ single-particle transition strength would overlap to some extent with the transitions contributing to the GDR. In fact, this overlap is evidenced by the dip in the $T_<$ distribution at 20 MeV in the calculation using the Soper interaction and at 21.5 MeV in the Tabakin case.

The measured integrated cross section up to 17 MeV (the region of the pygmy resonance) exhausts $(9.5 \pm 1.3)\%$ of the ^{17}O(γ,tot) cross section integrated up to 40 MeV. This compares with predictions using both the Soper and Tabakin interactions of 6.5% and with a value of 6% for the Kuo-Brown interaction; the strength below 20, 21.5, and 19 MeV, respectively, was taken as belonging to the pygmy resonance. The difference is understandable—the calculations place all of the dipole strength in the region below about 40 MeV, whereas in reality two-body correlations distribute some of the strength to much higher energies. As an indication of this, the integrated ^{17}O(γ,tot) cross section up to 40 MeV exhausts only 59% of the TRK sum-rule value. Particle-hole shell-model calculations seem to be capable of placing an adequate fraction of the total $E1$ absorption strength into the pygmy resonance by involving only the $1d_{5/2} \rightarrow 1f$-$2p$ single-particle transitions. There is, therefore, no need to invoke more sophisticated treatments involving the core to explain the observed pygmy strength.

G. Isospin splitting of core-excited GDR states of ^{17}O

The particle-hole shell-model calculations, discussed above, all predict that about $\frac{1}{3}$ of the energy-integrated (γ,tot) strength is from $T_<$ states and about $\frac{2}{3}$ from $T_>$ states. In all cases the center of the dipole strength from $T_<$ states is displaced lower in energy by a few MeV relative to that for the $T_>$ distribution. The resulting isospin splitting, defined by [22,75] $\Delta E = E_> - E_<$ ($E = \sigma_0/\sigma_{-1}$) is 3.7, 3.0, 4.1, and 3.4 MeV for the Soper, Tabakin, Cooper-Eisenberg, and Kuo-Brown interactions, respectively. Various other estimates for isospin splitting are available for ^{17}O: Two phenomenological-model estimates differ widely—one [75] gives 5.3 MeV and relates the magnitude of the isospin splitting to the symmetry energy of the nucleus, which another [21] gives a value of 1.8 MeV and relates the splitting to the rms radii of neutrons and protons; an essentially model-

independent estimate [22] based on sum-rule limits for $T = \frac{1}{2}$ nuclei gives an upper limit of 3.4 MeV.

Although the isospin nature of most of the features observed in the (γ, tot) cross section has been identified, the strong overlap of resonances makes it difficult to extract the $T_<$ and $T_>$ distributions; the major uncertainty arises in the GDR region, where the $T_<$ strength carried by non-ground-state neutrons is not known. Clearly, there is no spectacular separation of isospin components of the core-excited states forming the main GDR. However, a small separation can be inferred from the photonuclear data in the region 20–30 MeV. The $T_<$ strength is centered at ~22 MeV [from the (γ, n_0) cross section], and the $T_>$ centroid is somewhere between the three-peak structure at ~23 MeV and the broad feature at ~28 MeV, both of which contain mostly $T_>$ strength. A separation of 2–3 MeV is reasonable, consistent with microscopic theory (when the pygmy-resonance strength is excluded) and with estimates reported in Refs. [21] and [22].

In ^{13}C the core-excited $T_<$ fragment is observed at ~21 MeV and is separated clearly from the main GDR strength at ~24.5 MeV [19]. If we assume that the isospin-splitting magnitude in ^{17}O is comparable to that in ^{13}C [21,22,75], then the $T_<$ core-excited fragment(s) from the major $T_>$ transitions in ^{17}O (at ~23 MeV) should be located at around 20 MeV. Perhaps the $T = \frac{1}{2}$ peak(s) observed in the present work just below the main GDR (at 19.3 and 20.3 MeV) represents the $T_<$ core-excited fragment(s).

VI. SUMMARY AND CONCLUSION

This paper reports the measurement of the ^{17}O$(\gamma, p)^{16}$N reaction cross section from threshold to an excitation energy of 43 MeV. The measurement represents the cross section for the (γ, p) reaction leading to the low-lying bound states in ^{16}N only; (γ, pn) strength is not included. Because of the almost pure 1p-1h nature of the final states in ^{16}N, it is concluded that the measured $E1$ strength resulting from the (dominant) semidirect reaction process is almost entirely 2p-1h in nature, with only configurations of the type $(\pi 1p_{1/2})^{-1}$ represented. Comparison with the previously reported photoneutron cross section indicates a relative increase in amplitude of the $(1p_{3/2})^{-1}$ components in the wave function of strong $E1$ states, with increasing excitation energy through the GDR. It is inferred that the (γ, pn) strength, which is included in the photoneutron cross section, is large and comparable to the (γ, p) strength reported here. On the basis of proton pickup reactions, it is inferred that the present cross section represents the total photoproton transition strength from the $1p_{1/2}$ subshell. A measure of the energy splitting of strength from transitions $1p_{1/2} \rightarrow 2s$-$1d$ and $1p_{3/2} \rightarrow 2s$-$1d$ of ~1.6 MeV is obtained.

Distinct resonances are observed in the ^{17}O$(\gamma, p)^{16}$N cross section. Using the present data, together with results from other reactions for this nucleus, it is possible to make spin, parity, and isospin assignments for the main features. Furthermore, comparing the resonance strength observed in the (γ, p) cross section with that observed in radiative capture of composite particles, it is concluded that 3p-2h components play a significant role in the GDR region (~22 MeV) and a dominant role in the structure of weaker peaks observed just below the main GDR strength (~19–21 MeV).

The most striking feature of the cross section is the pronounced structure observed at 15.06 MeV. We assign $T = \frac{3}{2}$ to the major strength in this peak. On the basis of its large width and asymmetry, we conclude that more than one state is excited. Evidence is presented that $M1$ transitions to the known $\frac{3}{2}^+$ level at 15.20 MeV and possibly the $\frac{7}{2}^+$ level at 15.37 MeV are contributing to this structure. Further study of these levels is needed to confirm their transition multipolarity and to determine their electromagnetic transition widths: Large-angle (e, e') reaction are particularly sensitive probes of $M1$ transitions.

The intermediate structure observed in the photoproton cross section for ^{17}O in the region of the GDR is remarkably similar to that for ^{16}O, indicating that the valence neutron in ^{17}O has only a weak influence on transitions from the ^{16}O core, in support of the weak-coupling hypothesis, but is very different from the situation for ^{18}O, where the two valence neutrons profoundly perturb the ^{16}O core. The trends observed in the photoproton cross sections of ^{16,17,18}O, which reflect transitions from the core, appear to be linked with changes in ground-state properties related to static deformation (viz., ground-state correlations and rms charge radii) of the oxygen isotopes.

The (γ, p) cross section reported here has been added to the previously measured photoneutron cross section to provide a good approximation to the total photoabsorption cross section for ^{17}O. The GDR of ^{17}O is located at ~23 MeV with a maximum strength of ~16 mb and a width of ~5.5 MeV. The photoabsorption cross section for ^{17}O is considerably smaller than that for either ^{16}O or ^{18}O. A satisfactory explanation for this anomaly did not result from examining the possibility of greater integrated strength at higher energies (about 40 MeV) for the case of ^{17}O.

Comparison with several particle-hole shell-model calculations performed in a 2p-1h and 1p basis using different residual interactions shows that the main features of the photoabsorption cross section, including the isospin distributions, are generally well predicted. In particular—and contrary to previous interpretations—it is found that the single-particle transitions of the type $1d_{5/2} \rightarrow 1f$-$2p$ can account for the strength observed in the pygmy-resonance region. This supports the single-particle nature of the pygmy resonance and the near-spectator role of the core in valence particle excitations. Overall, the calculation of Harakeh, Paul, and Gorodetzky using the Kuo-Brown interaction seems best for the description within the particle-hole framework of collective $E1$ strength distribution in the GDR of the mass-17 system.

Finally, an isosopin splitting of core-excited states (only) of about 2–3 MeV is indicated in ^{17}O.

ACKNOWLEDGMENTS

[1] J. W. Jury, B. L. Berman, D. D. Faul, P. Meyer, and J. G. Woodworth, Phys. Rev. C **21**, 503 (1980).

[2] See E. G. Fuller, Phys. Rep. **127**, 185 (1985), and references therein.

[3] I. Morrison (private communication); see P. R. Andrews et al., Nucl. Phys. **A459**, 317 (1986); J. P. Elliott and B. H. Flowers, Proc. R. Soc. London A **242**, 57 (1957).

[4] See R. A. Eramzhyan, B. S. Ishkhanov, I. M. Kapitanov, and V. G. Neudatchin, Phys. Rep. **136**, 229 (1986), and references therein.

[5] G. V. O'Rielly, D. Zubanov, and M. N. Thompson, Phys. Rev. C **40**, 59 (1989).

[6] C. C. Chang, E. M. Diener, and E. Ventura, Nucl. Phys. **A258**, 91 (1976).

[7] I. Linck, L. Kraus, and S. L. Blatt, Phys. Rev C **21**, 791 (1980).

[8] V. Gillet, M. A. Melkanoff, and J. Raynal, Nucl. Phys. **A97**, 631 (1967).

[9] C. M. Shakin and W. L. Wang, Phys. Rev. Lett. **26**, 902 (1971); W. L. Wang and C. M. Shakin, Phys. Rev. C **5**, 1898 (1972); J. R. Calarco, S. W. Wissink, M. Sasao, K. Wienhard, and S. S. Hanna, Phys. Rev. Lett. **39**, 925 (1977); W. J. O'Connell and S. S. Hanna, Phys. Rev. C **17**, 892 (1978); S. S. Hanna, in Nuclear Physics with Electromagnetic Interactions, Vol. 108 of Lecture Notes in Physics, edited by H. Arenhövel and D. Drechsel (Springer-Verlag, Mainz, 1979), p. 288.

[10] See, for example, D. F. Measday, A. B. Clegg, and P. S. Fisher, Nucl. Phys. **61**, 269 (1965).

[11] R. G. Johnson, B. L. Berman, K. G. McNeill, J. G. Woodworth, and J. W. Jury, Phys. Rev. C **20**, 27 (1979). The energy scale of this measurement has been corrected (see Ref. [50]).

[12] J. W. Jury, J. D. Watson, D. Rowley, T. W. Phillips, and J. G. Woodworth, Phys. Rev. C **32**, 1817 (1985); J. W. Jury (unpublished).

[13] See G. E. Brown, L. Castillejo, and J. A. Evans, Nucl. Phys. **22**, 1 (1961) and references therein; also, see Ref. [9].

[14] M. N. Harakeh, P. Paul, and Ph. Gorodetzky, Phys. Rev. C **11**, 1008 (1975).

[15] B. E. Norum, J. C. Bergstrom, and H. S. Caplan, Nucl. Phys. **A289**, 275 (1977).

[16] D. J. Albert, Anton Nagl, Jacob George, R. F. Wagner, and H. Überall, Phys. Rev. C **16**, 503 (1977).

[17] J. A. Eden and Y. I. Assafiri, Aust. J. Phys. **39**, 871 (1986); J. A. Eden (private communication).

[18] P. Paul, in Proceedings of the Conference on Photonuclear Reactions and Applications, Asilomar, 1973, edited by B. L. Berman (Lawrence Livermore Laboratory, University of California, Livermore, 1973), Vol. I.

[19] J. C. Bergstrom, Hall Crannell, F. J. Kline, J. T. O'Brien, J W. Lightbody, Jr., and S. P. Fivozinsky, Phys. Rev. C **4**, 1514 (1971); M. Marangoni, P. L. Ottaviani, and A. M. Saruis, Phys. Lett. **49B**, 253 (1974).

[20] K. G. McNeill. J. W. Jury, M. N. Thompson, B. L. Berman, and R. E. Pywell, Phys. Rev. C **43**, 489 (1991).

[21] Renzo Leonardi, Phys. Rev. Lett. **28**, 836 (1972).

[22] R. Leonardi and E. Lipparini, Phys. Rev. C **11**, 2073 (1975).

[23] See Ref. [24] for the list of published work in this series.

[24] D. J. McLean, M. N. Thompson, D. Zubanov, K. G. McNeill, B. L. Berman, and J. W. Jury, Phys. Rev. C **44**, 1137 (1991).

[25] B. L. Berman and S. C. Fultz, Rev. Mod. Phys. **47**, 713 (1975).

[26] D. D. Faul, Ph.D. thesis, Lawrence Livermore National Laboratory Report No. UCRL-53057, 1980 (unpublished).

[27] D. D. Faul, B. L. Berman, P. Meyer, and D. L. Olson, Phys. Rev. C **24**, 849 (1981).

[28] J. G. Woodworth, K. G. McNeill, J. W. Jury, R. A. Alvarez, B. L. Berman, D. D. Faul, and P. Meyer, Lawrence Livermore National Laboratory Report No. UCRL-77471, 1978 (unpublished).

[29] J. G. Woodworth, K. G. McNeill, J. W. Jury, R. A. Alvarez, B. L. Berman, D. D. Faul, and P. Meyer, Phys. Rev. C **19**, 1667 (1979).

[30] The photon-energy resolution was determined from the width (305 ± 30 keV) of the 15.11-MeV state ($\Gamma \sim 5.5$ keV) in the ^{13}C(γ,n) cross section [33] using a Gaussian fit (cf. the quoted [33] 240-keV width determined by using a Lorentzian fit). Correcting for the slight differences in the separation of slits used in the present measurement to that used in the measurement reported in Ref. [33] yields a width of ~ 320 keV, which is in precise agreement with that calculated at $E_\gamma = 15$ MeV by Bramblett et al. [31] for positrons with $\pm 1\%$ energy resolution incident on a 0.76-mm-thick beryllium target. The photon resolution at higher energies was therefore taken from Ref. [31].

[31] R. L. Bramblett, J. T. Caldwell, B. L. Berman, R. R. Harvey, and S. C. Fultz, Phys. Rev. **148**, 1198 (1966).

[32] R. E. Pywell, B. L. Berman, J. G. Woodworth, J. W. Jury, K. G. McNeill, and M. N. Thompson, Phys. Rev. C **32**, 384 (1985).

[33] J. W. Jury, B. L. Berman, D. D. Faul, P. Meyer, K. G. McNeill, and J. G. Woodworth, Phys. Rev. C **19**, 1684 (1979).

[34] F. Ajzenberg-Selove, Nucl. Phys. **A460**, 1 (1986), and references therein.

[35] Certificat D'Etalonnage, Laboratoire de Métrologie des Raynnements Ionisants, source type EHE 6, No. 91, Saclay, 1979.

[36] Program SAF, written by D. Zubanov, University of Melbourne, 1986. A Monte Carlo method is used similar to that reported by Y. S. Horowitz, S. Mordechai, and A.

Dubi, Nucl. Instrum. Methods **123**, 551 (1975).

[37] A. H. Wapstra and G. Audi, Nucl. Phys. **A432**, 55 (1985).

[38] P. L. Lee, Nucl. Instrum. Methods **144**, 363 (1977).

[39] J. A. Eden, M. N. Thompson, and D. Zubanov (unpublished).

[40] G. Mairle, G. J. Wagner, P. Doll, K. T. Knöpfle, and H. Breuer, Nucl. Phys. **A299**, 39 (1978).

[41] See, for example, P. Carlos, H. Beil, R. Bergère, B. L. Berman, A. Leprêtre, and A. Veyssière, Nucl. Phys. **A378**, 317 (1982).

[42] F. Hinterberger, P. Von Rossen, S. Cierjacks, G. Schmalz, D. Erbe, and B. Leugers, Nucl. Phys. **A352**, 93 (1981).

[43] A. Cunsolo, A. Foti, G. Immè, G. Pappalardo, G. Raciti, and N. Saunier, Lett. Nuovo Cimento **38**, 87 (1983).

[44] S. S. Hanna, in *Photonuclear Reactions I*, Vol. 61 of *Lecture Notes in Physics*, edited by S. Costa and C. Schaerf (Springer-Verlag, Berlin, 1977), p. 275.

[45] M. Gell-Mann and V. L. Telegdi, Phys. Rev. **91**, 169 (1953).

[46] C. Rangacharyulu, E. J. Ansaldo, D. Bender, A. Richter, and E. Spamer, Nucl. Phys. **A406**, 493 (1983).

[47] K. A. Snover, P. G. Ikossi, and T. A. Trainor, Phys. Rev. Lett. **43**, 117 (1979); G. Küchler, A. Richter, E. Spamer, W. Steffen, and W. Knüpfer, Nucl. Phys. **A406**, 473 (1983); D. Bender, A. Richter, E. Spamer, E. J. Ansaldo, C. Rangacharyulu, and W. Knüpfer, *ibid.* **A406**, 504 (1983).

[48] G. Cardella, A. Cunsolo, A. Foti, G. Immé, G. Pappalardo, G. Raciti, F. Rizzo, and N. Saunier, Lett. Nuovo Cimento **41**, 429 (1984).

[49] K. P. Artemov, V. Z. Gol'dberg, I. P. Petrov, V. P. Rudakov, I. N. Serikov, V. A. Timofeev, R. Wolski, and J. Szmider, Yad. Fiz. **28**, 288 (1978) [Sov. J. Nucl. Phys. **28**, 145 (1978)].

[50] J. W. Jury (unpublished); K. G. McNeill and J. W. Jury, Phys. Rev. C **42**, 2234 (1990).

[51] T. Mo, R. A. Blue, and H. R. Weller, Nucl. Phys. **A197**, 290 (1972).

[52] F. Boreli, Fizika (Zagreb) **2**, 97 (1970).

[53] R. M. Keyser, R. A. Blue, and H. R. Weller, Phys. Lett. **34B**, 602 (1971); Nucl. Phys. **A186**, 528 (1972).

[54] J. L. Honsaker, T. H. Hsu, W. J. McDonald, and G. C. Neils, Nucl. Phys. **A144**, 473 (1970).

[55] G. E. Brown and A. M. Green, Nucl. Phys. **75**, 401 (1966).

[56] D. Zubanov, R. A. Sutton, M. N. Thompson, and J. W. Jury, Phys. Rev C **27**, 1957 (1983).

[57] A. D. Bates, R. P. Rassool, E. A. Milne, M. N. Thompson, and K. G. McNeill, Phys. Rev. C **40**, 506 (1989).

[58] J. W. Jury, B. L. Berman, J. G. Woodworth, M. N. Thompson, R. E. Pywell, and K. G. McNeill, Phys. Rev. C **26**, 777 (1982).

[59] V. P. Denisov, L. A. Kul'chitskiĭ, and I. Ya. Chubukov, Yad. Fiz. **14**, 889 (1971) [Sov. J. Nucl. Phys. **14**, 497 (1972)].

[60] R. E. Pywell, B. L. Berman, J. W. Jury, J. G. Woodworth, K. G. McNeill, and M. N. Thompson, Phys. Rev. C **27**, 960 (1983).

[61] J. S. Levinger and H. A. Bethe, Phys. Rev. **78**, 115 (1950); J. S. Levinger, *ibid.* **84**, 43 (1951).

[62] B. L. Berman, R. Bergère, and P. Carlos, Phys. Rev. C **26**, 304 (1982).

[63] R. Ö, Akyüz, Phys. Lett. **90B**, 26 (1980).

[64] R. S. Hicks, Phys. Rev. C **25**, 695 (1982).

[65] Also, see discussion by B. L. Berman, D. D. Faul, R. A. Alvarez, and P. Meyer, Phys. Rev. Lett. **36**, 1441 (1976).

[66] G. Mairle, K. T. Knöpfle, P. Doll, H. Breuer, and G. J. Wagner, Nucl. Phys. **A280**, 97 (1977).

[67] B. S. Reehal and B. H. Wildenthal, Part. Nucl. **6**, 137 (1973).

[68] G. Mairle and G. J. Wagner, Nucl. Phys. **A253**, 253 (1975).

[69] R. P. Singhal, J. R. Moreira, and H. S. Caplan, Phys. Rev. Lett. **24**, 73 (1970); H. Miska, B. Norum, M. V. Hynes, W. Bertozzi, S. Kowalski, F. N. Rad, C. P. Sargent, T. Sasanuma, and B. L. Berman, Phys. Lett. **83B**, 165 (1979); also, for rms charge radii of ^{16,17}O, see J. C. Kim, R. S. Hicks, R. Yen, I. P. Auer, H. S. Caplan, and J. C. Bergstrom, Nucl. Phys. **A297**, 301 (1978).

[70] D. Zubanov, M. N. Thompson, B. L. Berman, J. W. Jury, R. E. Pywell, and K. G. McNeill, University of Melbourne Report No. UM-P-89/43, 1989.

[71] See, for example, J. L. DuBard and R. K. Sheline, Phys. Rev. **182**, 1320 (1969); and A. de Shalit and H. Feshbach, *Theoretical Nuclear Physics* (Wiley, New York, 1974).

[72] H. P. Jolly, Jr., Phys. Lett. **5**, 289 (1963).

[73] Y. I. Assafiri and I. Morrison, Nucl. Phys. **A427**, 460 (1984).

[74] B. R. Easlea, Phys. Lett. **1**, 163 (1962).

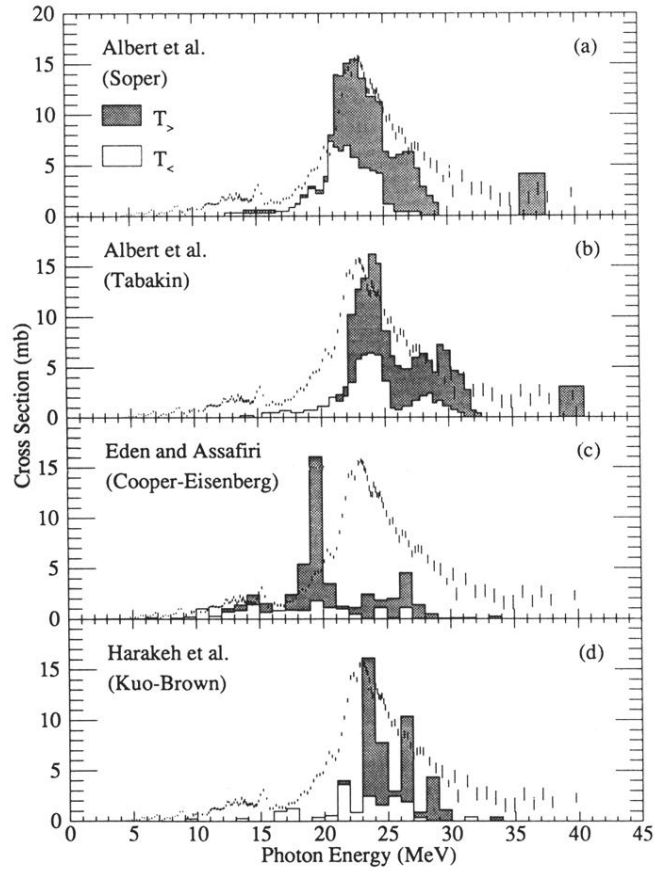[75] R. Ö. Akyüz and S. Fallieros, Phys. Rev. Lett. **27**, 1016 (1961).

FIG. 10. Comparison between the $^{17}O(\gamma,\text{tot})$ cross section $[\sigma(\gamma,\text{tot})\simeq\sigma(\gamma,p)+\sigma(\gamma,sn)]$ and several theoretical predictions: (a) that of Albert *et al.* [16] using a modified zero-range Soper interaction, (b) that of Albert *et al.* [16] using a Tabakin potential, (c) that of Eden and Assafiri [17] using the Cooper-Eisenberg interaction, and (d) that of Harakeh, Paul, and Gorodetzky [14] using the Kuo-Brown interaction.